Available online at www.sciencedirect.com
SCIENCE DIRECT
Advances in Water Resources 29 (2006) 1000–1019
Advances in Water Resources
www.elsevier.com/locate/advwatres

Diffusive wave solutions for open channel flows with uniform and concentrated lateral inflow

P. Fan *, J.C. Li

Institute of Mechanics, Chinese Academy of Sciences, No. 15 Beisihuanxi Road, Beijing 100080, China

Received 4 October 2004; received in revised form 31 August 2005; accepted 31 August 2005
Available online 13 October 2005

Abstract

The diffusive wave equation with inhomogeneous terms representing hydraulics with uniform or concentrated lateral inflow into a river is theoretically investigated in the current paper. All the solutions have been systematically expressed in a unified form in terms of response function or so called *K*-function. The integration of *K*-function obtained by using *Laplace* transform becomes *S*-function, which is examined in detail to improve the understanding of flood routing characters. The backwater effects usually resulting in the discharge reductions and water surface elevations upstream due to both the downstream boundary and lateral inflow are analyzed. With a pulse discharge in upstream boundary inflow, downstream boundary outflow and lateral inflow respectively, hydrographs of a channel are routed by using the *S*-functions. Moreover, the comparisons of hydrographs in infinite, semi-infinite and finite channels are pursued to exhibit the different backwater effects due to a concentrated lateral inflow for various channel types.

Keywords: Diffusive wave; Analytical solution; *Laplace* transformation; Backwater effect; Flood routing

1. Introduction

The quasi-linear hyperbolic *Saint-Venant* equation system (*Saint-Venant*, 1871) is generally used to describe unsteady flows in a river. Since rare analytical solution is available in most practical situations, the resolution of them mainly relies on numerical approaches based on either the characteristic lines [1], finite difference schemes [2,6,15], or finite volume method [29,13].

Within the framework of the original *Saint-Venant* equations, river hydraulics may be classified as dynamic, gravity, diffusion or kinematic wave models, corresponding to different forms of the momentum equation, respectively [10,33,8]. Dynamic wave model retains all the terms of the momentum equation, whereas gravity wave model neglects the effects of bed slope and viscous energy loss and describes flows that are dominated by inertia. As a matter of fact, the acceleration terms in the *Saint-Venant* equations can be neglected in most practical applications of flood routing in natural channels. The system is thus reduced to a single parabolic equation known as the diffusive wave model [25]. If the water depth gradient term is further omitted, the kinematic wave equation is acquired. The criteria for demarcating kinematic wave and diffusive wave have been fully discussed recently [22,23,26–28,20]. Cappelaere [5] devised a new method to improve the accuracy of the general nonlinear diffusive wave approach. Finally, solutions of the full diffusion wave model can be simulated by the *Muskingum–Cunge* (M–C) method [24]. It is shown that the solutions of the diffusion wave equation following the M–C approach always give accurate results once a straightforward condition is imposed [3]. In *Barry*'s study, the results are found to be of the

* Corresponding author. Tel.: +86 10 62554125; fax: +86 10 62561284.
E-mail address: fanping@imech.ac.cn (P. Fan).

0309-1708/$ - see front matter
doi:10.1016/j.advwatres.2005.08.008

Nomenclature

B	river width [m]
$\cos(\cdot)$	cosine function
C	celerity of diffusive wave [m/s]
D	diffusive coefficient for diffusive wave [m^2/s]
$\text{erf}(\cdot)$	error function
$\exp(\cdot)$	exponent function
$f(x,t)$	source term in Eq. (3)
$F_s(x,t)$	defined in Eq. (97)
Fr	the Froud number
g	the gravitational acceleration [m/s^2]
h	water depth [m]
$H(\cdot)$	Heaviside function
$K_0(x,\xi,t)$	defined in Eq. (8)
$K_u(x,t)$	kernel function relating to the upstream inflow
$K_d(x,t)$	kernel function relating to the downstream outflow
$K_l(x,t)$	kernel function relating to the lateral inflow
L	channel length
n	iteration number
$N(n)$	defined in Eq. (63)
p	*Laplace* variable
q	the discharge per unit width [m^2/s]
q_l	the lateral inflow per unit area of the confluent surface [m/s]
Q	discharge [m^3/s]
Q_0, Q_u, Q_d, Q_l	discharge for initial condition, upstream, downstream boundary conditions and lateral inflow respectively
$\tilde{Q}_u$, $\tilde{Q}_d$	*Laplace* transform of Q_u and Q_d respectively
R	defined in Eq. (73)
S_0	the bed slope
S_f	the friction slope
$S_u(x,t)$	S-function relating to the upstream inflow
$S_d(x,t)$	S-function relating to the downstream outflow
$S_l(x,t)$	S-function relating to the lateral inflow
$\sin(\cdot)$	sinusoidal function
t	time [s]
t_0	duration for the pulse inflow input [s]
T_0	flood duration
u_l	the velocity component of lateral inflow in the mainstream flow direction [m/s]
v	the mean cross-sectional velocity [m/s]
x	spatial coordinate [m]
x_0, x_1, x_2	coordinates of the confluent point, two sides of the confluent region, respectively [m]
$X(x)$, $T(t)$	defined in Eq. (10)
φ	defined in Eq. (68)
$\tilde{\varphi}$	*Laplace* transform of φ
$\delta(\cdot)$	Dirac delta function
ξ, u, η, τ	dummy integration variable
$*$	the convolution operation
L	*Laplace* transformation operation
L^{-1}	inverse *Laplace* transformation operation

second-order accuracy if the Courant number happens to be 1/2. Moreover, the accuracy criteria for the linearized diffusion routing problem are discussed by Bajracharya [4]. Both the spatial weighting factor and the time step are selected judiciously in this study to obtain guaranteed second-, third-, and fourth-order accurate schemes.

As an approximation, the diffusive wave model for unsteady flow routing has been used more frequently in recent years, since it may yield satisfactory solutions and reasonably account for the downstream backwater effect. As is well known, the diffusive wave equation can be solved analytically if celerity and diffusivity are assumed constant. Up to now, a number of analytical solutions for the diffusion equation have been derived under the hypotheses of negligible inhomogeneous term or without uniformly distributed lateral inflow [17,11,19,28]. Therefore, the application of previous solutions is very limited and not applicable in most of the practical circumstances for river networks system. Earlier analytical works scarcely considered the influences of various inflows. Hayami [17] initially presented the famous *Hayami* solution with the assumptions that the channel reach is semi-infinite only with an upstream boundary condition specified and the inhomogeneous term is omitted in the governing equations. Consequently, the disadvantage of *Hayami* model is obvious in that the backwater effects of downstream boundary and lateral inflow are ignored. Dooge et al. [11], Dooge and Napiorkowski [12] provided a solution of a finite channel, in which backwater effects of the lateral inflow were also neglected. Tawatchai and Shyam [30] derived analytical results in terms of water depth for a finite channel with a concentrated lateral inflow, which was applied to route the floods in a hypothetical rectangular channel with different upstream, downstream, and lateral boundary conditions and also showed good results when applied to simulate flood flow conditions in 1980 and 1981 in the Lower Mun River, in Northeast Thailand. An excellent means was hence provided by this model to analyze individual or overall effects of the boundary conditions and much less effort and time were required at a particular station. Chung et al. [7] used numerical inverse *Laplace* transform to study the backwater effect of the downstream boundary in a finite channel. Based on the *Hayami*'s solution, Moussa [19] developed a method in order to solve the diffusive wave equation with a lateral inflow or outflow uniformly distributed over a channel reach. Unfortunately, this solution is still based on the hypothesis of a semi-infinite channel and thus unable to study the influences of downstream boundary and concentrated lateral inflow. Singh [28] presented more overall solutions, except for cases with a concentrated lateral inflow. On the other hand, the characteristics of response functions have not been fully discussed. Moramarco et al. [18] obtained the analytical solutions by linearizing the full *Saint-Venant* equations with uniform lateral inflow. Fan et al. [14] yielded a solution for an infinite channel with a concentrated lateral inflow and compared it with the numerical solutions. It can be seen that more general solutions of the diffusive wave model with source terms in various types of channel have not been given thus far. And different backwater effects from the downstream boundary and the lateral inflow need further systematic exploration as well.

In the present paper, analytical methods are developed to derive general solutions in a unified form of expression in terms of kernel functions applicable for infinite, semi-infinite and finite channels with concentrated and uniform lateral inflows. At the same time, the hydrographs reflecting flood routing process in different cases are carefully examined with *S*-functions given.

2. General solution of the diffusive wave equation

The classic *Saint-Venant* equations for one-dimensional, unsteady, open-channel flow in a rectangular channel can be written in the form,

$$\frac{\partial h}{\partial t}+\frac{\partial q}{\partial x}=\frac{q_1}{B} \tag{1}$$

$$\frac{\partial q}{\partial t}+\frac{\partial}{\partial x}\left(\frac{q^2}{h}+\frac{gh^2}{2}\right)=gh(S_0-S_f)+q_1\frac{u_1}{B} \tag{2}$$

where h is the water depth, q the discharge per unit width, B the river width, t the time, x the distance along the flow direction. q_1 denotes the lateral inflow per unit width of the confluent region. S_0 is the bed slope, S_f the friction slope, g the gravitational acceleration, u_1 the velocity component of lateral inflow in the mainstream flow direction.

Neglecting the inertia term as $Fr^2 \ll 1$ and eliminating variable h from Eq. (1) and (2), a single diffusive wave equation with a source term in terms of discharge $Q = qB$ can be rendered as (see Appendix E),

$$\frac{\partial Q}{\partial t}+C\frac{\partial Q}{\partial x}=D\frac{\partial^2 Q}{\partial x^2}+f(x,t) \tag{3}$$

in which,

$$C=\frac{1}{B}\frac{dQ}{dh} \tag{4}$$

$$D=\frac{Q}{2BS_f}\approx\frac{Q}{2BS_0} \tag{5}$$

where C and D are the diffusion wave celerity and diffusion coefficient, respectively, Q the discharge. The inhomogeneous term in Eq. (3) looks like,

$$f(x,t)=Cq_1-D\frac{\partial q_1}{\partial x} \tag{6}$$

The characteristic scale for flood diffusion in a channel is found to be proportional to $\sqrt{(DT_0)}$, where T_0 is the flood duration. Accordingly, a channel can be specified as finite, infinite or semi-infinite by comparing scales of the channel length L and of the flood diffusion $\sqrt{(DT_0)}$. Supposing that the distance between upstream water source and downstream sink (such as lake or estuary) $L \sim \sqrt{(DT_0)}$, the channel is usually regarded as finite and hence the boundary conditions at two ends should be imposed. In contrast, a channel is assumed semi-infinite or infinite provided that $L \gg \sqrt{(DT_0)}$, in which only one or neither boundary condition need consideration (see Fig. 1). In the following text, we are concerned with diffusive waves in above-mentioned three kinds of channel forms with uniformly distributed or concentrated lateral inflows.

2.1. Diffusive waves in infinite channels

In an infinite channel, the upstream and downstream boundary conditions are usually ignored and the initial condition is specified as,

$$Q(x,t)|_{t=0}=Q_0(x),\quad -\infty < x < +\infty \tag{7}$$

The solution of Eq. (3) in infinite space can readily be acquired (see Appendix A) as,

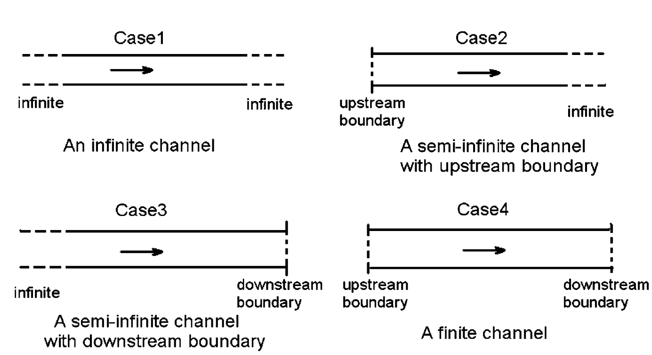

Fig. 1. Sketches for the four kinds of channel types, in which case 1, case 2, case 3 and case 4 represents an infinite channel, a semi-infinite channel with upstream boundary, a semi-infinite channel with downstream boundary and a finite channel, respectively.

$$Q(x,t) = \int_{-\infty}^{+\infty} Q_0(\xi) K_0(x,\xi,t)\,\mathrm{d}\xi + \int_{-\infty}^{+\infty} f(\xi,t) * K_0(x,\xi,t)\,\mathrm{d}\xi \tag{8}$$

in which,

$$K_0(x,\xi,t) = \frac{1}{2\sqrt{\pi D t}} \exp\left(-\frac{(x-\xi-Ct)^2}{4Dt}\right) \tag{9}$$

where $*$ denotes the convolution operation.

In most circumstances, the temporal and spatial distributions of lateral inflow discharge $q_l(x,t)$ are usually independent. Thus $q_l(x,t)$ can be separated into a product of two factors as follows [19],

$$q_l(x,t) = X(x)T(t) \tag{10}$$

where $X(x)$ is the discharge distribution function in space, $T(t)$ implies the total discharge of the lateral inflow. Note that $q_l(x, t)$ has the dimension of discharge per width [m^2/s]. Accordingly the dimension of $X(x)$ is [1/m] and the dimension of $T(t)$ is identical to that of discharge [m^3/s].

By substituting Eq. (10) into Eq. (6), the source term in the original diffusive wave equation (3) can be represented as,

$$f(x,t) = T(t)\left[C \cdot X(x) - D\frac{\mathrm{d}}{\mathrm{d}x}X(x)\right] \tag{11}$$

The second term at the right hand of Eq. (8) is transformed into,

$$\int_{-\infty}^{\infty} f(\xi,t) * K_0(x,\xi,t)\,\mathrm{d}\xi = T(t) * \int_{-\infty}^{\infty}\left[C \cdot X(\xi) - D\frac{\mathrm{d}}{\mathrm{d}\xi}X(\xi)\right]K_0(x,\xi,t)\,\mathrm{d}\xi \tag{12}$$

Similar to the definition of the kernel function in *Hayami*'s solution [19], the kernel function (simplified to *K*-function in this paper) $K_l(x,t)$ relating to the lateral inflow discharge can be defined as,

$$K_l(x,t) = \int_{-\infty}^{\infty}\left[C \cdot X(\xi) - D\frac{\mathrm{d}}{\mathrm{d}\xi}X(\xi)\right]K_0(x,\xi,t)\,\mathrm{d}\xi \tag{13}$$

satisfying,

$$\int_{-\infty}^{\infty} f(\xi,t) * K_0(x,\xi,t)\,\mathrm{d}\xi = T(t) * K_l(x,t) \tag{14}$$

In reality, the lateral discharge into a channel is classified in two categories. One for the system of stream and aquifer [19,21] and the other describes channels with tributaries. The lateral inflow uniformly distributes along a river reach for the former, whereas the lateral inflow concentrates in the tributary for the latter (see Fig. 2). As a result, the distribution function $X(x)$ can be put in the following forms:

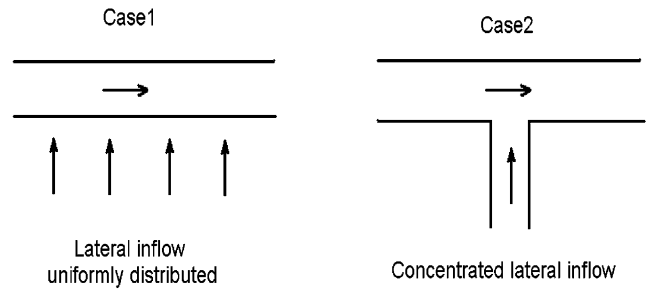

Fig. 2. Sketches for the channel with the two kinds of lateral inflow, in which case 1 and case 2 describe uniform and concentrated lateral inflows, respectively.

(i) For lateral inflows uniformly distributed in the region $[x_1, x_2]$, the distribution function $X(x)$ can be written as,

$$X(x,x_1,x_2) = \frac{H(x-x_1) - H(x-x_2)}{x_2 - x_1} = \begin{cases} \frac{1}{x_2-x_1} & x \in [x_1,x_2] \\ 0 & x \notin [x_1,x_2] \end{cases} \tag{15}$$

in which *Heaviside* function satisfies,

$$H(x-x_1) = \begin{cases} 1 & x \geqslant x_1 \\ 0 & x < x_1 \end{cases} \tag{16}$$

(ii) For a lateral inflow concentrated at point x_0 (assuming the width of the tributary negligible) the distribution function $X(x)$ satisfies,

$$X(x) = \delta(x-x_0) = \begin{cases} \infty & x = x_0 \\ 0 & x \neq x_0 \end{cases} \tag{17}$$

in which $\delta(x)$ is the Dirac function.

2.1.1. Diffusive waves with a uniform lateral inflow

By substituting Eqs. (15) and (9) into Eq. (13) we have expression of the *K*-function $K_l(x,t)$ for the lateral inflow uniformly distributed in region $[x_1, x_2]$ as follows:

$$\begin{aligned} K_l(x,t) &= \frac{C}{x_2-x_1}\int_{x_1}^{x_2} K_0(x,\xi,t)\,\mathrm{d}\xi + \frac{D}{x_2-x_1}[K_0(x,x_2,t) - K_0(x,x_1,t)] \\ &= \frac{-C}{2(x_2-x_1)}\left[\mathrm{erf}\left(\frac{x-x_2-Ct}{2\sqrt{Dt}}\right) - \mathrm{erf}\left(\frac{x-x_1-Ct}{2\sqrt{Dt}}\right)\right] + \frac{\sqrt{D}}{2\sqrt{\pi t}(x_2-x_1)} \\ &\quad \times \left[\exp\left(-\frac{(x-x_2-Ct)^2}{4Dt}\right) - \exp\left(-\frac{(x-x_1-Ct)^2}{4Dt}\right)\right] \end{aligned} \tag{18}$$

in which $\mathrm{erf}(x)$ is the Error function.

The *K*-function is essentially the same as the instantaneous unit hydrograph (IUH), the integration of which is customarily called the storage function [9,32]. As the hydrograph at any location of a channel can be routed directly by the storage function, more interests in the present paper hence are laid on the storage function (hereafter simply called *S*-function) than IUH. For instance, if the discharge process and *S*-function for a lateral inflow input are defined as $Q_l(x,t)$ and $S_l(x,t)$ respectively, the lateral inflow is approximated by histograms as [30],

$$T(t) = T_j, \quad j-1 < t \leqslant j, \ j = 1,\ldots,n \tag{19}$$

Then the discharge process induced by the lateral inflow input satisfies,

$$Q_l(x,t) = T_1 S_l(x,t) + \sum_{j=1}^{n} S_l(x,t-j)(T_{j+1} - T_j) \tag{20}$$

where the definition of $S_l(x,t)$ for the lateral inflow is written as below,

$$S_l(x,t) = \int_0^t K_l(x,\tau)\,\mathrm{d}\tau = 1 * K_l(x,t) \tag{21}$$

It shows from the above expression that *S*-function represents the flood routing process with a continuous unit input. With parameters set as $C = 1$ m/s, $D = 10{,}000$ m^2/s (the values of C and D remain unchanged henceforth unless they are specified additionally), $x_1 = 5$ km and $x_2 = 10$ km, $S_l(x,t)$ are illustrated in Fig. 3(a), while the limits of which are depicted in Fig. 3(b). Fig. 3(a) shows that, (a) $S_l(x,t)$ is negative for $x < x_1$ and approximates to zero as time tends to infinity; Each curve has a minimum which diminishes as x approaches to x_1; (b) $S_l(x,t)$ increases with t for $x > x_2$ and decreases with x; Each curve has the common limit, unit; (c) The limits of $S_l(x,t)$ rise with the coordinates for $x_1 < x < x_2$. Consequently, we may lead to the conclusion that the lateral inflow not only propagates downstream but also results in the discharge reduction upstream, which is usually called backwater effect. In the confluent region, $S_l(x,t)$ rises with the coordinates. Conversely, $S_l(x,t)$ reduces with distance out of the confluent region, which is apparently characteristic of diffusive waves. With a continuous unit input, the flood waves die out and the steady flow state recovers as time approaches to infinity.

Using characters of the *Laplace* transformation gives,

$$\mathrm{L}[K_0(x,\xi,t)]|_{p=0} = \frac{1}{C}\exp\left(\frac{C(x-\xi-|x-\xi|)}{2D}\right) = \begin{cases} \frac{1}{C} & x > \xi \\ \frac{1}{C}\exp\left(\frac{C(x-\xi)}{D}\right) & x < \xi \end{cases} \tag{22}$$

in which L represents the *Laplace* transformation operator. Accordingly, the limit of $S_l(x,t)$ can be calculated in the following way:

$$\begin{aligned} \lim_{t\to\infty} S_l(x,t) &= \int_0^{\infty} K_l(x,\tau)\,\mathrm{d}\tau = \mathrm{L}[K_l(x,t)]|_{p=0} \\ &= \frac{C}{x_2-x_1}\int_{x_1}^{x_2} \mathrm{L}[K_0(x,\xi,t)]|_{p=0}\,\mathrm{d}\xi \\ &\quad + \frac{D}{x_2-x_1}[\mathrm{L}[K_0(x,x_2,t)]|_{p=0} - \mathrm{L}[K_0(x,x_1,t)]|_{p=0}] \\ &= \begin{cases} 1 & x > x_2 \\ \frac{x-x_1}{x_2-x_1} & x_1 < x < x_2 \\ 0 & x < x_1 \end{cases} \end{aligned} \tag{23}$$

It is clearly seen that the limits accords with what has shown in Fig. 3(b).

2.1.2. Diffusive waves with a concentrated lateral inflow

The expression of the *K*-function $K_l(x,t)$ for a lateral inflow concentrated at x_0 can be attained by substituting Eqs. (17) and (9) into Eq. (13),

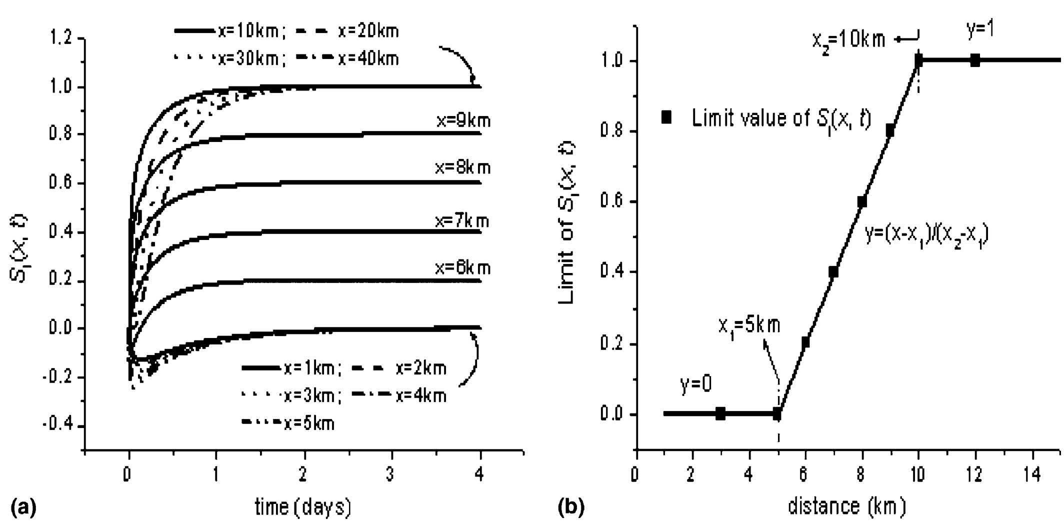

Fig. 3. (a) $S_l(x,t)$ for an infinite channel with a lateral inflow uniformly distributed in the region [5 km, 10 km]; (b) limits of $S_l(x,t)$ shown in (a).

$$K_1(x,t) = CK_0(x,x_0,t) + D\frac{\partial K_0(x,\xi,t)}{\partial \xi}\bigg|_{\xi=x_0} = \frac{x-x_0+Ct}{4\sqrt{\pi D t^3}}\exp\left(-\frac{(x-x_0-Ct)^2}{4Dt}\right) \quad (24)$$

Then the S-function is,

$$S_1(x,t) = \int_0^t \frac{x-x_0+C\tau}{4\sqrt{\pi D\tau^3}}\exp\left(-\frac{(x-x_0-C\tau)^2}{4D\tau}\right)d\tau = \begin{cases} \frac{1}{2}\left[1-\mathrm{erf}\left(\frac{x-x_0-Ct}{2\sqrt{Dt}}\right)\right] & \stackrel{t\to\infty}{\to} 1, \quad x > x_0 \\ \frac{1}{2}\mathrm{erf}\left(\frac{C\sqrt{t}}{2\sqrt{D}}\right) & \stackrel{t\to\infty}{\to} \frac{1}{2}, \quad x = x_0 \\ \frac{1}{2}\left[\mathrm{erf}\left(\frac{x_0-x+Ct}{2\sqrt{Dt}}\right)-1\right] & \stackrel{t\to\infty}{\to} 0, \quad x < x_0 \end{cases} \quad (25)$$

Comparing Eq. (25) to Eq. (23), they are different in that the limit of $S_1(x,t)$ is 1/2 at the confluent point $x = x_0$.

Usually, the discharge reductions and water surface elevations upstream due to the downstream constrictions such as the reservoir and piers are termed as the downstream backwater effect. This effect generating a steady and spatially gradually varying water surface profile gives rise to serious impacts on the sediments transport and flood prevention in a river [30,31]. Actually, a backwater effect may be generated as well by the lateral inflow for a river, which is usually ignored however. In the current paper, the negative minimum values of $S_1(x,t)$ is used to scale the backwater effect due to the lateral inflow. The following two equations evaluate the zero point of the first order and the second order derivatives of $S_1(x,t)$.

$$\frac{\partial}{\partial t}\left[\mathrm{erf}\left(\frac{x_0-x+Ct}{2\sqrt{Dt}}\right)\right]\bigg|_{t=\frac{x_0-x}{C}} = \left(-\frac{x_0-x-Ct}{4\sqrt{Dt^3}}\right)e^{-\left(\frac{x_0-x+Ct}{2\sqrt{Dt}}\right)^2}\bigg|_{t=\frac{x_0-x}{C}} = 0 \quad (26)$$

$$\frac{\partial^2}{\partial t^2}\left[\mathrm{erf}\left(\frac{x_0-x+Ct}{2\sqrt{Dt}}\right)\right]\bigg|_{t=\frac{x_0-x}{C}} = \left[\frac{8Dt[3(x_0-x)-Ct]-(x_0-x+Ct)(x_0-x-Ct)^2}{16\sqrt{D^3t^7}} \times e^{-\left(\frac{x_0-x+Ct}{2\sqrt{Dt}}\right)^2}\right]\bigg|_{t=\frac{x_0-x}{C}} > 0 \quad (27)$$

As a result, the minimum value of $S_1(x,t)$ for $x < x_0$ is,

$$\mathrm{Min}[S_1(x,t)] = \frac{1}{2}\left[\mathrm{erf}\left(\frac{x_0-x+Ct}{2\sqrt{Dt}}\right)-1\right]\bigg|_{t=\frac{x_0-x}{C}} = -\frac{1}{2}\left|1-\mathrm{erf}\left(\sqrt{\frac{C(x_0-x)}{D}}\right)\right| \quad (28)$$

which indicates that the minimum value of $S_1(x,t)$ decreases with $|x_0 - x|$. Therefore, we may conclude that the backwater effect is intensified as moving close to the confluent point and reaches maximum right at the confluent point $x = x_0$.

2.1.3. Hydrographs for a concentrated lateral inflow input

Traditionally used for flood routing process study by hydrologists, the hydrographs due to different inputs including lateral inflow, upstream inflow and downstream outflow are investigated as well in the current paper. The lateral inflow distributed along the river reach uniformly or even varying in space very probably becomes a more interesting problem and needs further study. Hence, only hydrographs due to a concentrated lateral inflow are considered here. A pulse input from a concentrated lateral inflow $T(t)$ can be set as follows:

$$T(t) = \begin{cases} 1 & t \leqslant t_0 \\ 0 & t > t_0 \end{cases}, \quad t_0 = 7200\ \mathrm{s} \quad (29)$$

in which $T(t)$ is unit for $t < t_0$ and zero for $t > t_0$ ($t_0 = 2$ h). Hydrograph for the concentrated lateral inflow input can be governed by,

$$Q_1(x,t) = \int_0^t T(\tau)K_1(x,t-\tau)d\tau = \begin{cases} S_1(x,t) & t \leqslant t_0 \\ S_1(x,t) - S_1(x,t-t_0) & t > t_0 \end{cases} \quad (30)$$

If neglecting the initial condition, hydrograph for an infinite channel with a concentrated lateral inflow input is illustrated in Fig. 4. It shows that the flood quantity from a tributary not only propagates in the downstream direction but also causes a backwater effect resulting in the discharge reduction in the upstream direction. Both

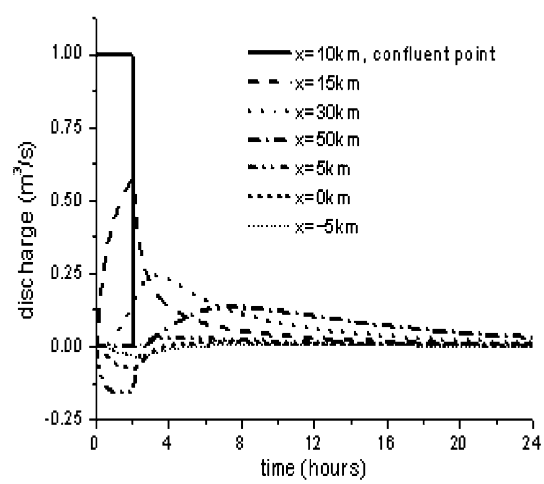

Fig. 4. Hydrographs for an infinite channel with a pulse input from a lateral inflow concentrated at $x_0 = 10$ km.

the discharges propagated in the downstream direction and the backwater effect in the upstream direction attenuate with the distance from the confluent point.

2.1.4. Sensitivity analysis of parameters C and D

The graphs for various celerity C and diffusivity D are plotted in Figs. 5–7, where C varies from 0.5 to 2 m/s and D from 10,000 to 100,000 m^2/s, respectively. In Fig. 5 hydrographs are compared at $x = 0$ km ($x - x_0 < 0$), showing that the backwater effect decreases with C and increases with D. Fig. 6 shows that the flood peak increases with C and reduces with D for $x = 15$ km ($0 < x - x_0 < Ct_0 = 7.2$ km). In contrast, for $x = 30$ km and $x - x_0 > Ct_0$ in Fig. 7, the flood peak rises with both C and D. All of these conclusions (summarized in Table 1) can also be explained by Eq. (25).

2.2. Diffusive waves in semi-infinite channels with upstream boundary

For a semi-infinite channel with upstream boundary, the boundary condition of the original diffusion equation is specified as,

$$Q(x,t)|_{x=0} = Q_u(t), \quad 0 \leqslant t < +\infty \tag{31}$$

together with the initial condition,

$$Q(x,t)|_{t=0} = Q_0(x), \quad 0 \leqslant x < +\infty \tag{32}$$

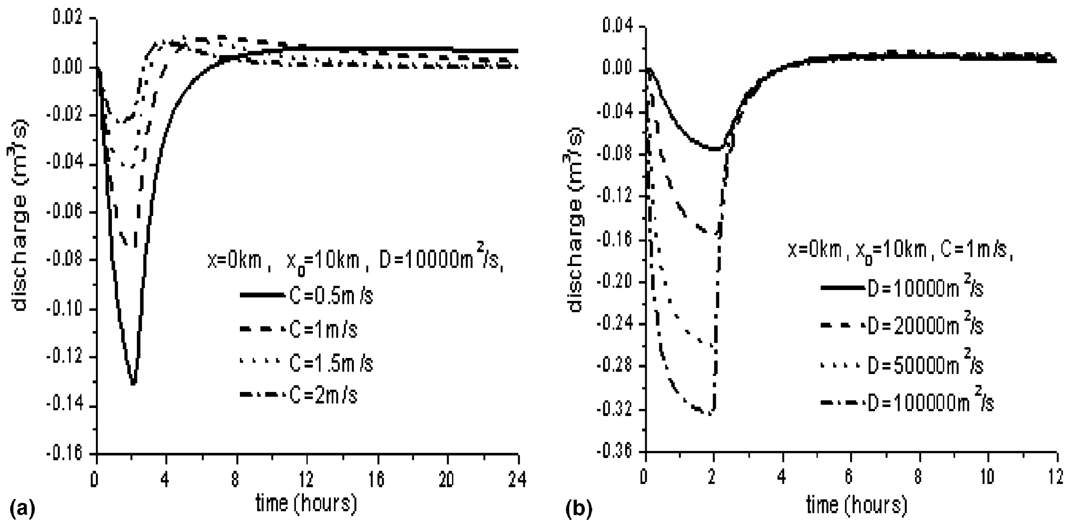

Fig. 5. Comparisons of hydrographs at $x = 0$ km for an infinite channel with a pulse input from a lateral inflow concentrated at $x_0 = 10$ km; (a) D is fixed at 10,000 m^2/s and C ranges from 0.5 to 2 m/s; (b) C is fixed at 1 m/s and D ranges from 10,000 to 100,000 m^2/s.

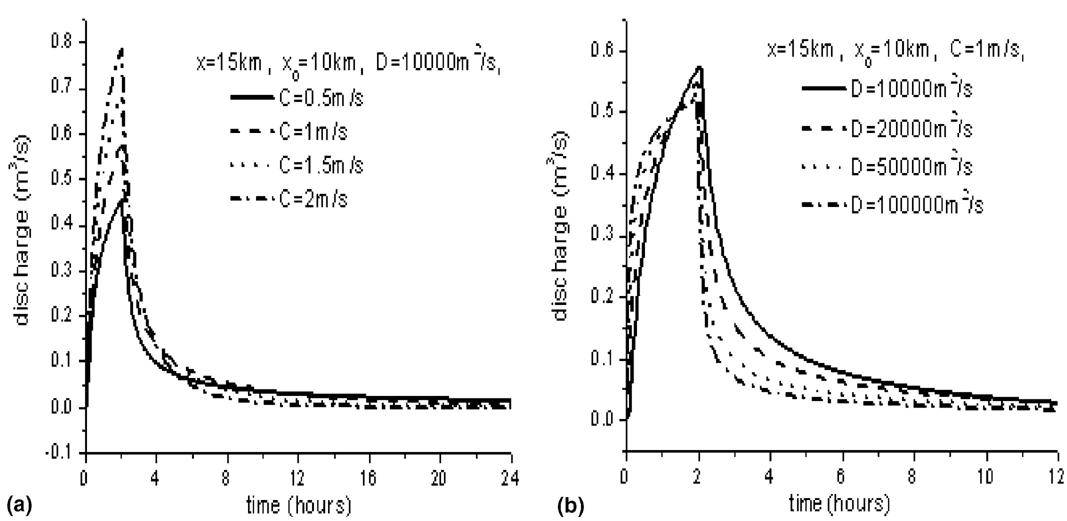

Fig. 6. Comparisons of hydrographs at $x = 15$ km for an infinite channel with a pulse input from a lateral inflow concentrated at $x_0 = 10$ km; (a) D is fixed at 10,000 m^2/s and C ranges from 0.5 to 2 m/s; (b) C is fixed at 1 m/s and D ranges from 10,000 to 100,000 m^2/s.

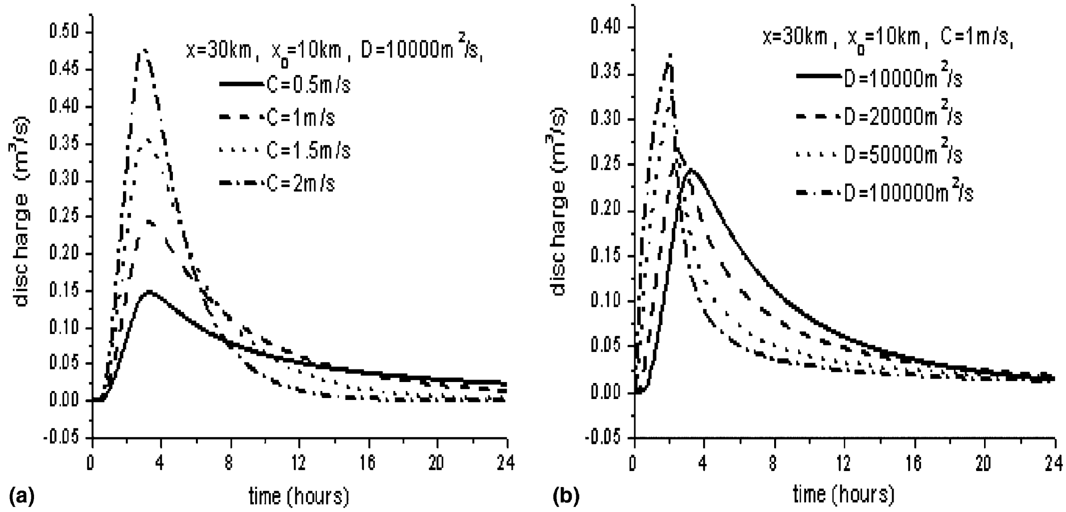

Fig. 7. Comparisons of hydrographs at $x = 30$ km for an infinite channel with a pulse input from a lateral inflow concentrated at $x_0 = 10$ km; (a) D is fixed at 10,000 m^2/s and C ranges from 0.5 to 2 m/s; (b) C is fixed at 1 m/s and D ranges from 10,000 to 100,000 m^2/s.

Table 1
Effects of increasing parameter C and D on characters of flood wave

Flood character	Only C increases			Only D increases		
	Upstream	Downstream		Upstream	Downstream	
		$x - x_0 < Ct_0$	$x - x_0 > Ct_0$		$x - x_0 < Ct_0$	$x - x_0 > Ct_0$
Backwater effect	Decrease			Increase		
Flood peak		Increase	Increase		Decrease	Increase

Upstream and downstream denotes the direction of diffusive waves.
Note: Reverse condition occurs when C and D decrease.

The solution in the semi-infinite space can be derived (see Appendix B) as,

$$Q(x,t) = Q_u(t) * K_u(x,t) + \int_0^{\infty} Q_0(\xi) K_0(x,\xi,t)\,d\xi + \int_0^{\infty} f(\xi,t) * K_0(x,\xi,t)\,d\xi \quad (33)$$

where,

$$K_u(x,t) = \frac{x}{2\sqrt{\pi D} t^{3/2}} \exp\left(-\frac{(x-Ct)^2}{4Dt}\right) \quad (34)$$

$$K_0(x,\xi,t) = \frac{1}{2\sqrt{\pi D t}}\left[\exp\left(-\frac{(x-\xi-Ct)^2}{4Dt}\right) - \exp\left(\frac{Cx}{D}\right)\exp\left(-\frac{(x+\xi+Ct)^2}{4Dt}\right)\right] \quad (35)$$

Obviously $K_u(x,t)$ is the K-function for the upstream boundary inflow.

2.2.1. Diffusive waves with a upstream inflow

Note that the K-function $K_u(x,t)$ is essentially the same as the solution obtained by Hayami [17]. The S-function for $K_u(x,t)$ is written as below,

$$\begin{aligned} S_u(x,t) &= \int_0^t K_u(x,\tau)\,d\tau \\ &= \int_0^t \frac{x + C\tau}{4\sqrt{\pi D \tau^3}} \exp\left(-\frac{(x-C\tau)^2}{4D\tau}\right) d\tau + \exp\left(\frac{Cx}{D}\right)\int_0^t \frac{x - C\tau}{4\sqrt{\pi D \tau}} \exp\left(-\frac{(x+C\tau)^2}{4D\tau}\right) d\tau \\ &= \frac{1}{2}\left[1 - \operatorname{erf}\left(\frac{x-Ct}{2\sqrt{Dt}}\right)\right] + \frac{1}{2}\exp\left(\frac{Cx}{D}\right) \times \left[1 - \operatorname{erf}\left(\frac{x+Ct}{2\sqrt{Dt}}\right)\right] \overset{t\to\infty}{\to} 1 \end{aligned} \quad (36)$$

which shows the unit limit of $S_u(x,t)$ as time approaching to infinity. It can be concluded from Fig. 8(a) as well. The curves in Fig. 8(a) representing $S_u(x,t)$ for a semi-infinite channel with upstream boundary have the common limit, unit, and reduce along with the channel reach.

2.2.2. Diffusive waves with a uniform lateral inflow

For a lateral inflow uniformly distributed in region $[x_1, x_2]$, the K-function $K_l(x,t)$ can be obtained by substituting Eq. (35) into Eq. (18) as follows:

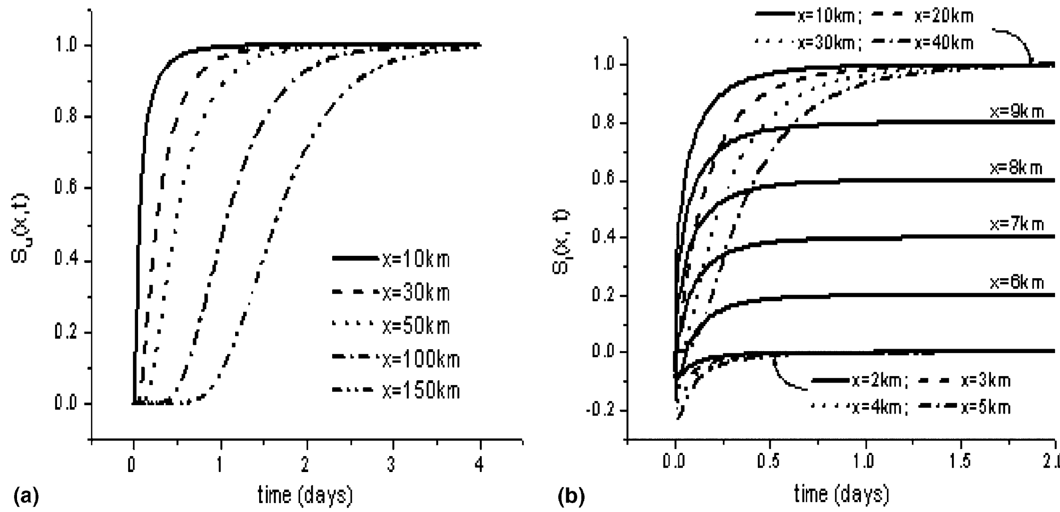

Fig. 8. *S*-functions for a semi-infinite channel with the upstream boundary at $x = 0$ km; (a) $S_u(x,t)$ for a upstream inflow; (b) $S_l(x,t)$ for a lateral inflow uniformly distributed in region [5 km, 10 km].

$$\begin{aligned}K_l(x,t) &= \frac{C}{x_2-x_1}\int_{x_1}^{x_2} K_0(x,\xi,t)\,\mathrm{d}\xi \\ &\quad + \frac{D}{x_2-x_1}[K_0(x,x_2,t)-K_0(x,x_1,t)] \\ &= \frac{-C}{2}\frac{\operatorname{erf}\left(\frac{x-x_2-Ct}{2\sqrt{Dt}}\right)-\operatorname{erf}\left(\frac{x-x_1-Ct}{2\sqrt{Dt}}\right)}{x_2-x_1} \\ &\quad + \frac{C}{2}\exp\left(\frac{Cx}{D}\right)\frac{\operatorname{erf}\left(\frac{x+x_2+Ct}{2\sqrt{Dt}}\right)-\operatorname{erf}\left(\frac{x+x_1+Ct}{2\sqrt{Dt}}\right)}{x_2-x_1} \\ &\quad + \frac{\sqrt{D}}{2\sqrt{\pi t}}\frac{\exp\left(-\frac{(x-x_2-Ct)^2}{4Dt}\right)-\exp\left(-\frac{(x-x_1-Ct)^2}{4Dt}\right)}{x_2-x_1} \\ &\quad - \frac{\sqrt{D}}{2\sqrt{\pi t}}\exp\left(\frac{Cx}{D}\right) \\ &\quad \times \frac{\exp\left(-\frac{(x+x_2+Ct)^2}{4Dt}\right)-\exp\left(-\frac{(x+x_1+Ct)^2}{4Dt}\right)}{x_2-x_1}\end{aligned} \tag{37}$$

Since Eq. (37) has not a more concise expression, therefore, the *S*-function can hardly find an analytical expression. Fig. 8(b) plots $S_l(x,t)$ exhibiting similar characteristics to that in Fig. 3(a).

2.2.3. Diffusive waves with a concentrated lateral inflow

The *K*-function for a lateral inflow concentrated at x_0 can be derived by substituting Eq. (35) into Eq. (24),

$$\begin{aligned}K_l(x,t) &= CK_0(x,x_0,t) + D\left.\frac{\partial K_0(x,\xi,t)}{\partial \xi}\right|_{\xi=x_0} \\ &= \begin{cases} \frac{x}{2\sqrt{\pi Dt^3}}\exp\left(-\frac{(x-Ct)^2}{4Dt}\right) = K_u(x,t) & x_0 = 0 \\ \frac{x-x_0+Ct}{4\sqrt{\pi Dt^3}}\exp\left(-\frac{(x-x_0-Ct)^2}{4Dt}\right) + \frac{x+x_0-Ct}{4\sqrt{\pi Dt^3}} & \\ \quad\times\exp\left(\frac{Cx}{D}\right)\exp\left(-\frac{(x+x_0+Ct)^2}{4Dt}\right) & x_0 > 0 \end{cases}\end{aligned} \tag{38}$$

Integrating the above equation gives,

$$S_l(x,t) = \begin{cases} x_0 = 0 & S_u(x,t) \\ x_0 > 0 & \begin{cases} \frac{1}{2}\left[1-\operatorname{erf}\left(\frac{x-x_0-Ct}{2\sqrt{Dt}}\right)\right] + \frac{1}{2}\exp\left(\frac{Cx}{D}\right) \\ \quad\times\left[1-\operatorname{erf}\left(\frac{x+x_0+Ct}{2\sqrt{Dt}}\right)\right] & x > x_0 \\ \frac{1}{2}\operatorname{erf}\left(\frac{C\sqrt{t}}{2\sqrt{D}}\right) + \frac{1}{2}\exp\left(\frac{Cx}{D}\right) \\ \quad\times\left[1-\operatorname{erf}\left(\frac{x+x_0+Ct}{2\sqrt{Dt}}\right)\right] & x = x_0 \\ \frac{1}{2}\left[\operatorname{erf}\left(\frac{|x-x_0|+Ct}{2\sqrt{Dt}}\right)-1\right] + \frac{1}{2}\exp\left(\frac{Cx}{D}\right) \\ \quad\times\left[1-\operatorname{erf}\left(\frac{x+x_0+Ct}{2\sqrt{Dt}}\right)\right] & x < x_0 \end{cases} \end{cases} \tag{39}$$

It is clearly seen that the above function has the same limit as Eq. (25). Comparing Eqs. (39) and (25) leads to differences of $S_l(x,t)$ for the cases that the channel is infinite and semi-infinite with upstream boundary as follows:

$$\Delta S_l(x,t) = \frac{1}{2}\exp\left(\frac{Cx}{D}\right)\left[1-\operatorname{erf}\left(\frac{x+x_0+Ct}{2\sqrt{Dt}}\right)\right] \tag{40}$$

in which $\Delta S_l(x,t)$ stands for the influence of the upstream boundary on the flow due to lateral inflow input. As $\Delta S_l(x,t)$ is positive, the discharge induced by the lateral inflow input is always enlarged by the upstream boundary. For a certain flood duration t, if $x_0 \gg 2\sqrt{(Dt)}$, we have $\Delta S_l(x,t) \to 0$ as $x \to \infty$. Physically, it means that if the distance between the upstream boundary and the confluent point is long enough, influence of the upstream boundary vanishes.

2.2.4. Hydrographs for upstream boundary and concentrated lateral inflow inputs

By using the similar method as indicated in Eq. (30) ($S_l(x,t)$ in that equation should be replaced by $S_u(x,t)$ here), hydrographs with a pulse input from the upstream

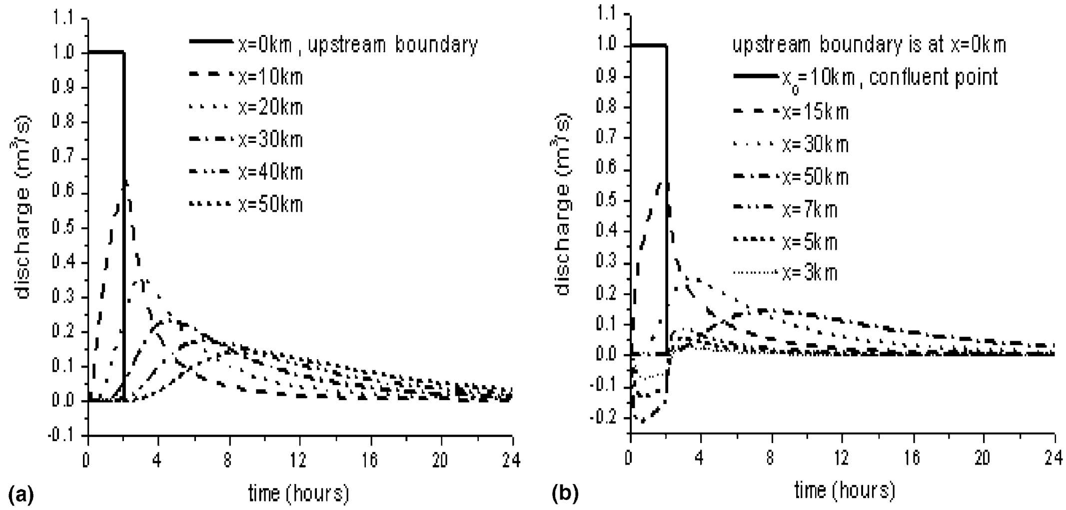

Fig. 9. Hydrographs for a semi-infinite channel with the upstream boundary at $x = 0$ km; (a) a pulse input from the upstream inflow; (b) a pulse input from the lateral inflow concentrated at $x_0 = 10$ km.

boundary are plotted in Fig. 9(a), showing the flood routing processes clearly from the upstream inflow input.

In the meantime, Fig. 9(b) shows the hydrograph with a pulse input from a concentrated lateral inflow in a semi-infinite channel, of which the backwater effect from the lateral inflow appears similar to that in Fig. 4. The differences are illustrated in Fig. 10, in which the hydrographs from a concentrated lateral inflow are compared for an infinite channel and semi-infinite channel with upstream boundary respectively. It can be inferred that the upstream boundary of the semi-infinite channel enlarges the discharges from the lateral inflow, meanwhile lessens the backwater effect of the lateral inflow.

2.3. Diffusive waves in semi-infinite channels with downstream boundary

For a semi-infinite channel with downstream boundary, the boundary condition and initial condition are as follows:

$$Q(x,t)|_{x=0} = Q_d(t), \quad -\infty < x \leqslant 0 \tag{41}$$

$$Q(x,t)|_{t=0} = Q_0(x), \quad -\infty < x \leqslant 0 \tag{42}$$

The solution in the semi-infinite space can be expressed (see Appendix C) as,

$$Q(x,t) = Q_d(t) * K_d(x,t) + \int_{-\infty}^{0} Q_0(\xi) K_0(x,\xi,t)\,d\xi + \int_{-\infty}^{0} f(\xi,t) * K_0(x,\xi,t)\,d\xi \tag{43}$$

where,

$$K_d(x,t) = \frac{|x|}{2\sqrt{\pi D} t^{3/2}} \exp\left(-\frac{(|x|+Ct)^2}{4Dt}\right) \tag{44}$$

and $K_0(x,\xi,t)$ is identical to Eq. (35).

2.3.1. Diffusive waves with downstream outflow

Integrating the K-function $K_d(x,t)$ gives the S-function for the downstream outflow $S_d(x,t)$ as follows:

$$\begin{aligned} S_d(x,t) &= \int_0^t \frac{|x| - C\tau}{4\sqrt{\pi D \tau^3}} \exp\left(-\frac{(|x|+C\tau)^2}{4D\tau}\right) d\tau \\ &\quad + \exp\left(-\frac{C|x|}{D}\right) \int_0^t \frac{|x| + C\tau}{4\sqrt{\pi D \tau}} \\ &\quad \times \exp\left(-\frac{(|x|-C\tau)^2}{4D\tau}\right) d\tau \\ &= \frac{1}{2}\left[1 - \operatorname{erf}\left(\frac{|x|+Ct}{2\sqrt{Dt}}\right)\right] \\ &\quad + \frac{1}{2}\exp\left(-\frac{C|x|}{D}\right)\left[1 - \operatorname{erf}\left(\frac{|x|-Ct}{2\sqrt{Dt}}\right)\right] \end{aligned} \tag{45}$$

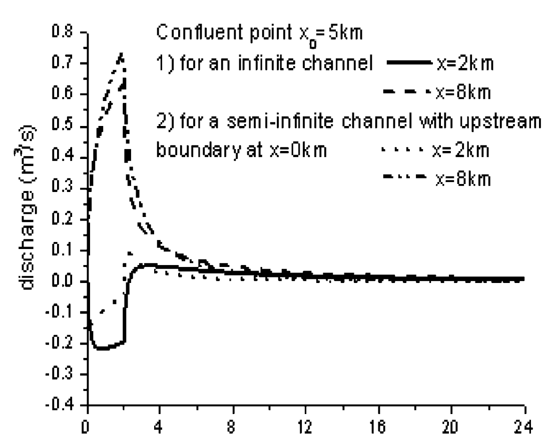

Fig. 10. Comparisons of hydrographs for the cases that the channel is infinite and semi-infinite with upstream boundary at $x = 0$ km respectively; a pulse input from the lateral inflow concentrated at $x_0 = 5$ km.

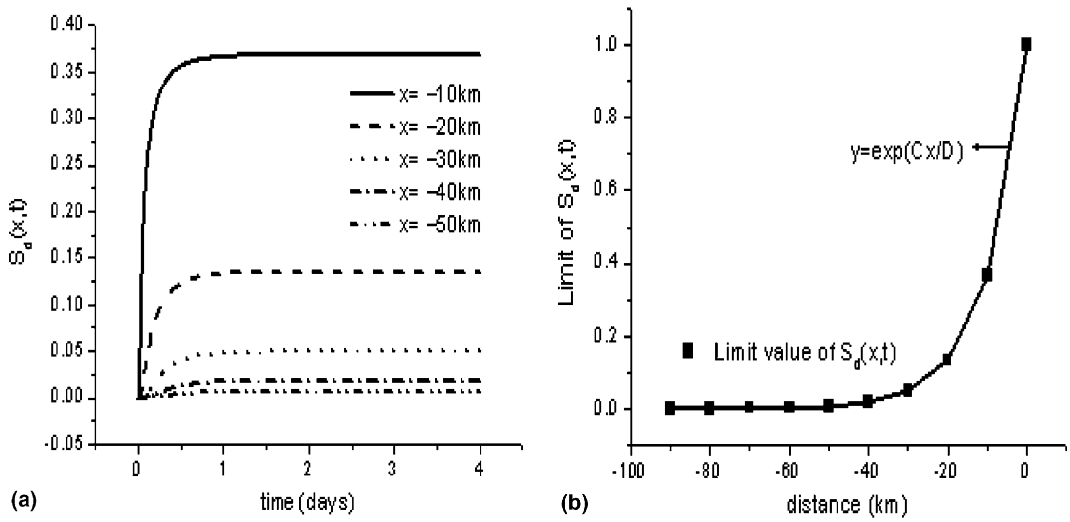

Fig. 11. (a) $S_d(x,t)$ for a semi-infinite channel with downstream boundary at $x=0$ km; (b) limits of $S_d(x,t)$ in (a).

which is plotted in Fig. 11(a). $S_d(x,t)$ are always positive, implying that the discharge in a channel rises due to an outflow at the downstream boundary. Moreover, the induced discharge reduces as moving away from the downstream boundary. Fig. 11(b) illustrates the limit of the curves in Fig. 11(a), which satisfies $\exp(Cx/D)$. By using *Laplace* transformation, the limit of $S_d(x,t)$ is expressed as,

$$\begin{aligned}\lim_{t\to\infty} S_d(x,t) &= \mathrm{L}[K_d(x,t)]|_{p=0} \\ &= \exp\left(\frac{Cx}{2D}\right)\exp\left(-\frac{|x|}{\sqrt{D}}\sqrt{p+\frac{C^2}{4D}}\right)\Bigg|_{p=0} \\ &= \exp\left(\frac{Cx}{D}\right) \end{aligned} \tag{46}$$

which is found in agreement with the diagrams in Fig. 11(b).

2.3.2. Diffusive waves with a uniform lateral inflow

Since $K_0(x,\xi,t)$ is identical to Eq. (35), the *K*-function $K_l(x,t)$ with a lateral inflow uniformly distributed in region $[x_1,x_2]$ has the same expression as Eq. (37). The *S*-function $S_l(x,t)$ now is plotted in Fig. 12(a), where the curves show different characters from those in Fig. 3(a) or Fig. 8(b). It indicates an important fact that due to the different integral regions, the expression of $S_l(x,t)$ for a semi-infinite channel with upstream boundary differs from that with downstream boundary, even if the *K*-functions in each case are the same. Fig. 12(a) also demonstrates that (a) for $x<x_1$ $S_l(x,t)$ are negative and decreases with time; Each curve has a negative limit which diminishes to zero as x tends to infinity; (b) for

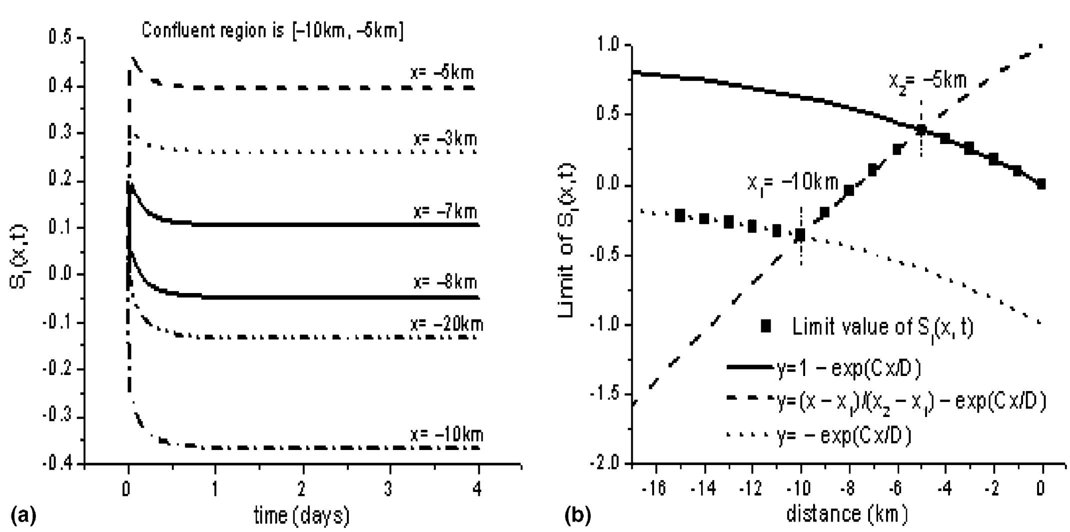

Fig. 12. (a) $S_l(x,t)$ for a semi-infinite channel with a lateral inflow uniformly distributed in region [−10 km, −5 km], the downstream boundary at $x=0$ km; (b) limits of $S_l(x,t)$ in (a).

$x > x_2$ $S_l(x,t)$ increases at first and decreases with time subsequently; Each curve has a positive limit which diminishes to zero at the downstream boundary $x = 0$ km; (c) for $x_1 < x < x_2$ the limits of $S_l(x,t)$ increase with the coordinate. Hence it shows that the downstream boundary exerts different influence on the flow of the lateral inflow from the upstream boundary. The upstream boundary always amplifies the discharge due to the lateral inflow input, while the downstream boundary reduces the discharge.

The *Laplace* transformation of $K_0(x,\xi,t)$ gives,

$$\mathrm{L}[K_0(x,\xi,t)] = \frac{1}{2\sqrt{D}}\exp\left(\frac{C(x-\xi)}{2D}\right)\frac{1}{\sqrt{p+\frac{C^2}{4D}}} \times \left[\exp\left(-\frac{|x-\xi|}{\sqrt{D}}\sqrt{p+\frac{C^2}{4D}}\right) - \exp\left(-\frac{|x+\xi|}{\sqrt{D}}\sqrt{p+\frac{C^2}{4D}}\right)\right] \tag{47}$$

And the limit of $S_l(x,t)$ for lateral inflow uniformly distributed in region $[x_1,x_2]$ can be given as,

$$\lim_{t\to\infty} S_l(x,t) = \begin{cases} 1-\exp\left(\frac{Cx}{D}\right) & x > x_2 \\ \frac{x-x_1}{x_2-x_1} - \exp\left(\frac{Cx}{D}\right) & x_1 \leqslant x \leqslant x_2 \\ -\exp\left(\frac{Cx}{D}\right) & x < x_1 \end{cases} \tag{48}$$

As compared with Eq. (23), we may find that the difference between them happens to be $\exp(Cx/D)$, namely, the limit of $S_d(x,t)$ in Eq. (46), which implies that Eq. (48) exhibits the superposition of effects of lateral inflow and downstream boundary. Fig 12(b) plots the limit of $S_l(x,t)$ and displays the strongest backwater effect occurring at $x = x_1$.

2.3.3. Diffusive waves with a concentrated lateral inflow

By using similar approach to Eq. (38), the K-function $K_l(x,t)$ for lateral inflow concentrated at x_0 can be obtained as follows:

$$K_l(x,t) = CK_0(x,x_0,t) + D\left.\frac{\partial K_0(x,\xi,t)}{\partial \xi}\right|_{\xi=x_0} = \begin{cases} \frac{x}{2\sqrt{\pi D t^3}}\exp\left(-\frac{(x-Ct)^2}{4Dt}\right) = -K_d(x,t) & x_0 = 0 \\ \frac{x-x_0+Ct}{4\sqrt{\pi D t^3}}\exp\left(-\frac{(x-x_0-Ct)^2}{4Dt}\right) + \frac{x+x_0-Ct}{4\sqrt{\pi D t^3}}\exp\left(\frac{Cx}{D}\right) \times \exp\left(-\frac{(x+x_0+Ct)^2}{4Dt}\right) & x_0 < 0 \end{cases} \tag{49}$$

the integration of which leads to the S-function as below,

$$S_l(x,t) = \begin{cases} x_0 = 0 & -S_d(x,t) \\ x_0 < 0 & \begin{cases} \frac{1}{2}\left[1-\mathrm{erf}\left(\frac{|x-x_0|-Ct}{2\sqrt{Dt}}\right)\right] + \frac{1}{2}\exp\left(\frac{Cx}{D}\right) \times \left[\mathrm{erf}\left(\frac{|x+x_0|-Ct}{2\sqrt{Dt}}\right) - 1\right] & x > x_0 \\ \frac{1}{2}\mathrm{erf}\left(\frac{C\sqrt{t}}{2\sqrt{D}}\right) + \frac{1}{2}\exp\left(\frac{Cx}{D}\right) \times \left[\mathrm{erf}\left(\frac{|x+x_0|-Ct}{2\sqrt{Dt}}\right) - 1\right] & x = x_0 \\ \frac{1}{2}\left[\mathrm{erf}\left(\frac{|x-x_0|+Ct}{2\sqrt{Dt}}\right) - 1\right] + \frac{1}{2}\exp\left(\frac{Cx}{D}\right) \times \left[\mathrm{erf}\left(\frac{|x+x_0|-Ct}{2\sqrt{Dt}}\right) - 1\right] & x < x_0 \end{cases} \end{cases} \tag{50}$$

and the limitation turns out,

$$\lim_{t\to\infty} S_l(x,t)|_{x_0<0} = \begin{cases} 1-\exp\left(\frac{Cx}{D}\right) & x > x_0 \\ \frac{1}{2}-\exp\left(\frac{Cx}{D}\right) & x = x_0 \\ -\exp\left(\frac{Cx}{D}\right) & x < x_0 \end{cases} \tag{51}$$

It is clearly seen that the K-functions $K_l(x,t)$ for a semi-infinite channel with downstream boundary Eq. (49) is the same as that with the upstream boundary Eq. (38). However, Eq. (50) differs from Eq. (25) significantly. The difference of the two $S_l(x,t)$ for $x_0 < 0$ is,

$$\Delta S_l'(x,t) = \frac{1}{2}\exp\left(\frac{Cx}{D}\right)\left[\mathrm{erf}\left(\frac{|x+x_0|-Ct}{2\sqrt{Dt}}\right) - 1\right] \tag{52}$$

There is a slight difference between the above equation and Eq. (40), which shows the downstream boundary generates different influences on the flow of the lateral inflow input from the upstream boundary. $\Delta S_l'(x,t)$ is always negative indicating that the discharge induced by the lateral inflow input is reduced by the downstream boundary. Furthermore, this effect appears to vanish if the distance between the downstream boundary and the confluent point is long enough.

2.3.4. Hydrographs for the downstream boundary outflow and concentrated lateral inflow

Hydrographs for a pulse outflow from downstream boundary are plotted in Fig. 13(a). It shows that an outflow from the downstream boundary also enlarges the discharges of a semi-infinite channel. Actually, if a reservoir is regarded as the downstream boundary of a channel in the upland, the increasing of outflow from this reservoir is equivalent to the rise of discharge and hence leads to the descending of the water stage.

Hydrographs for a pulse input from a concentrated lateral inflow in a semi-infinite channel are shown in Fig. 13(b), of which the implications are analogous to that revealed in Fig. 4. The differences between the two cases are shown in Fig. 14. We may conclude that the downstream boundary exerts an opposite influence on the flow of a lateral inflow input as compared to the upstream boundary cases. In other words, the

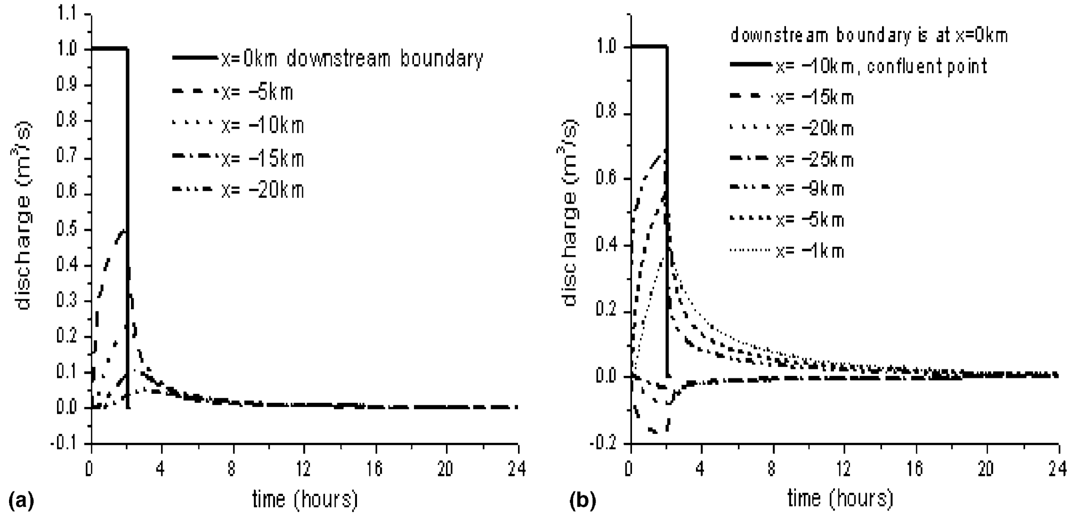

Fig. 13. Hydrographs for a semi-infinite channel with downstream boundary at $x = 0$ km; (a) a pulse input from the downstream outflow; (b) a pulse input from the lateral inflow concentrated at $x_0 = -10$ km.

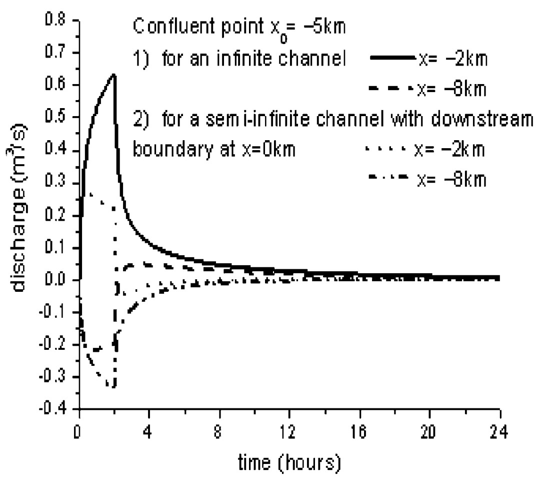

Fig. 14. Comparisons of hydrographs for the channel is infinite and semi-infinite with downstream boundary at $x = 0$ km respectively; a pulse input from the lateral inflow concentrated at $x_0 = -5$ km.

backwater effect of the lateral inflow is intensified by the downstream boundary.

2.4. Diffusive waves in finite channels

Boundary conditions for a finite channel are usually described as,

$$Q(x,t)|_{x=0} = Q_{\mathrm{u}}(t), \quad Q(x,t)|_{x=L} = Q_{\mathrm{d}}(t) \tag{53}$$

and the initial condition is,

$$Q(x,t)|_{t=0} = Q_0(x) \tag{54}$$

Then, the solution of a finite channel can be obtained (see Appendix D) as,

$$\begin{aligned} Q(x,t) &= Q_{\mathrm{u}}(t) * K_{\mathrm{u}}(x,t) + Q_{\mathrm{d}}(t) * K_{\mathrm{d}}(x,t) \\ &\quad + \int_0^L Q_0(\xi) K_0(x,\xi,t)\,\mathrm{d}\xi \\ &\quad + \int_0^L f(\xi,t) * K_0(x,\xi,t)\,\mathrm{d}\xi \end{aligned} \tag{55}$$

in which,

$$\begin{aligned} K_{\mathrm{u}}(x,t) &= \exp\left(\frac{Cx}{2D} - \frac{C^2 t}{4D}\right) \\ &\quad \times \sum_{n=1}^{+\infty} \frac{2n\pi D}{L^2} \exp\left(-\frac{n^2\pi^2 D}{L^2} t\right) \sin\frac{n\pi x}{L} \end{aligned} \tag{56}$$

$$\begin{aligned} K_{\mathrm{d}}(x,t) &= \exp\left(\frac{C(x-L)}{2D} - \frac{C^2 t}{4D}\right) \\ &\quad \times \sum_{n=1}^{+\infty} \frac{2n\pi D}{L^2} (-1)^{n+1} \exp\left(-\frac{n^2\pi^2 D}{L^2} t\right) \sin\frac{n\pi x}{L} \end{aligned} \tag{57}$$

$$\begin{aligned} K_0(x,\xi,t) &= \exp\left(\frac{C(x-\xi)}{2D} - \frac{C^2 t}{4D}\right) \frac{2}{L} \\ &\quad \times \sum_{n=1}^{+\infty} \exp\left(-\frac{n^2\pi^2 D}{L^2} t\right) \sin\frac{n\pi\xi}{L} \sin\frac{n\pi x}{L} \end{aligned} \tag{58}$$

2.4.1. Diffusive waves with the upstream inflow and downstream outflow

Both K-function $K_{\mathrm{u}}(x,t)$ and $K_{\mathrm{d}}(x,t)$ with the upstream inflow and downstream outflow are found to be identical to those obtained by Dooge et al. [11] and Singh [28]. Subsequently, the S-functions $S_{\mathrm{u}}(x,t)$ and $S_{\mathrm{d}}(x,t)$ are derived in the following way:

$$S_{\mathrm{u}}(x,t) = \int_0^t K_{\mathrm{u}}(x,\tau)\,\mathrm{d}\tau = \exp\left(\frac{Cx}{2D}\right)\sum_{n=1}^{+\infty}\frac{8n\pi D^2}{(C^2L^2+4n^2\pi^2D^2)} \times\left(1-\exp\left(-\frac{C^2L^2+4n^2\pi^2D^2}{4DL^2}t\right)\right)\sin\frac{n\pi x}{L} \quad (59)$$

$$S_{\mathrm{d}}(x,t) = \int_0^t K_{\mathrm{d}}(x,\tau)\,\mathrm{d}\tau = \exp\left(\frac{C(x-L)}{2D}\right)\sum_{n=1}^{+\infty}\frac{(-1)^{n+1}8n\pi D^2}{(C^2L^2+4n^2\pi^2D^2)} \times\left(1-\exp\left(-\frac{C^2L^2+4n^2\pi^2D^2}{4DL^2}t\right)\right)\sin\frac{n\pi x}{L} \quad (60)$$

2.4.2. Diffusive waves with a uniform lateral inflow

Substituting Eq. (58) into Eq. (18) gives the K-function $K_{\mathrm{l}}(x,t)$ for the lateral inflow uniformly distributed in region $[x_1,x_2]$,

$$K_{\mathrm{l}}(x,t) = \exp\left(\frac{Cx}{2D}-\frac{C^2t}{4D}\right)\frac{2}{L} \times\sum_{n=1}^{+\infty}N(n)\exp\left(-\frac{n^2\pi^2D}{L^2}t\right)\sin\frac{n\pi x}{L} \quad (61)$$

integration of which leads to,

$$S_{\mathrm{l}}(x,t) = \int_0^t K_{\mathrm{l}}(x,\tau)\,\mathrm{d}\tau = \exp\left(\frac{Cx}{2D}\right)\frac{2}{L}\sum_{n=1}^{+\infty}\frac{4DL^2N(n)}{4n^2\pi^2D^2+C^2L^2} \times\left[1-\exp\left(-\frac{4n^2\pi^2D^2+C^2L^2}{4DL^2}t\right)\right]\sin\frac{n\pi x}{L} \quad (62)$$

where,

$$N(n) = \frac{2D}{(x_2-x_1)(1+(\frac{2D}{C}\frac{n\pi}{L})^2)} \times\left[\frac{(\frac{2D}{C}\frac{n\pi}{L})^2-1}{2}\left(\sin\left(\frac{n\pi x_2}{L}\right)\exp\left(-\frac{Cx_2}{2D}\right) - \sin\left(\frac{n\pi x_1}{L}\right)\exp\left(-\frac{Cx_1}{2D}\right)\right) + \frac{2D}{C}\frac{n\pi}{L}\left(\cos\left(\frac{n\pi x_1}{L}\right)\exp\left(-\frac{Cx_1}{2D}\right) - \cos\left(\frac{n\pi x_2}{L}\right)\exp\left(-\frac{Cx_2}{2D}\right)\right)\right] \quad (63)$$

2.4.3. Diffusive waves with a concentrated lateral inflow

The K-function $K_{\mathrm{l}}(x,t)$ and S-function $S_{\mathrm{l}}(x,t)$ with the lateral inflow concentrated at x_0 can be obtained by substituting Eq. (57) into Eq. (24), as follows:

$$K_{\mathrm{l}}(x,t) = CK_0(x,x_0,t) + D\left.\frac{\partial K_0(x,\xi,t)}{\partial\xi}\right|_{\xi=x_0} = \exp\left(\frac{C(x-x_0)}{2D}-\frac{C^2t}{4D}\right)\sum_{n=1}^{+\infty}\exp\left(-\frac{n^2\pi^2D}{L^2}t\right) \times\left(\frac{C}{L}\sin\frac{n\pi x_0}{L}+\frac{2n\pi D}{L^2}\cos\frac{n\pi x_0}{L}\right)\sin\frac{n\pi x}{L} \quad (64)$$

$$S_{\mathrm{l}}(x,t) = \exp\left(\frac{C(x-x_0)}{2D}\right)\sum_{n=1}^{+\infty}\frac{4DL^2}{4n^2\pi^2D^2+C^2L^2} \times\left[1-\exp\left(-\frac{4n^2\pi^2D^2+C^2L^2}{4DL^2}t\right)\right] \times\left(\frac{C}{L}\sin\frac{n\pi x_0}{L}+\frac{2n\pi D}{L^2}\cos\frac{n\pi x_0}{L}\right)\sin\frac{n\pi x}{L} \quad (65)$$

For the extreme instance that confluent point is at $x_0 = 0$, $K_{\mathrm{l}}(x,t)$ can be simplified into,

$$K_{\mathrm{l}}(x,t) = \exp\left(\frac{Cx}{2D}-\frac{C^2t}{4D}\right) \times\sum_{n=1}^{+\infty}\frac{2n\pi D}{L^2}\exp\left(-\frac{n^2\pi^2D}{L^2}t\right)\sin\frac{n\pi x}{L} = K_{\mathrm{u}}(x,t) \quad (66)$$

and for $x_0 = L$, simplified as,

$$K_{\mathrm{l}}(x,t) = \exp\left(\frac{C(x-L)}{2D}-\frac{C^2t}{4D}\right) \times\sum_{n=1}^{+\infty}\frac{2n\pi D}{L^2}(-1)^n\exp\left(-\frac{n^2\pi^2D}{L^2}t\right)\sin\frac{n\pi x}{L} = -K_{\mathrm{d}}(x,t) \quad (67)$$

The above two equations are similar to Eqs. (38) and (49), which indicates that the lateral inflow seems to propagate downstream when a lateral inflow concentrates at the upstream boundary and the backwater effect occurs when it concentrates at the downstream boundary.

2.4.4. Hydrographs for a concentrated lateral inflow input

The hydrograph of diffusive waves with a lateral inflow input concentrated at $x_0 = 10$ km in a finite channel of the length 20 km is plotted in Fig. 15, in which the whole flood process is clearly exhibited. Fig. 16 compares the hydrograph at $x = 15$ km in three cases: the channels are as long as 20 km, 50 km and semi-infinite channel without downstream boundary, respectively. It shows that the hydrograph of lateral inflow input is

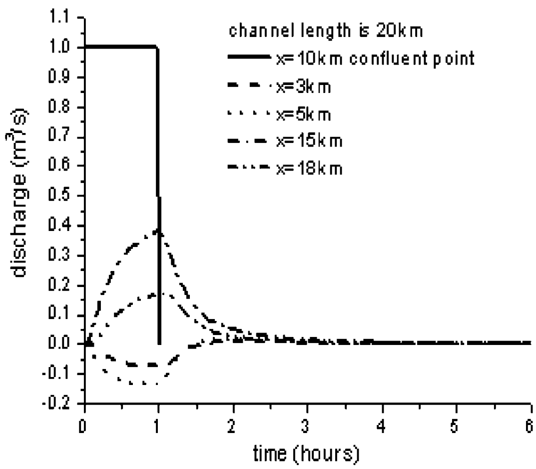

Fig. 15. Hydrographs for a finite channel with upstream and downstream boundary at $x = 0$ km and $x = 20$ km respectively; a pulse input comes from the lateral inflow concentrated at $x_0 = 10$ km.

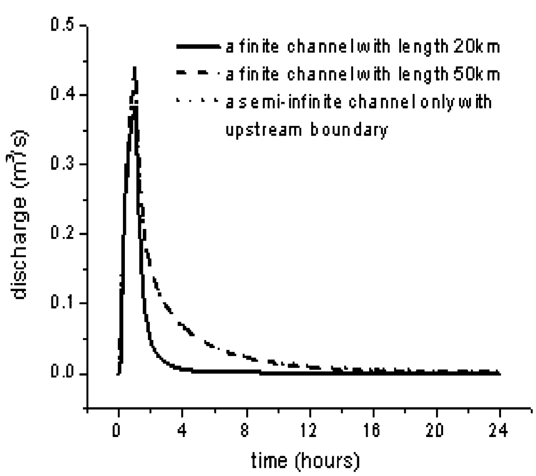

Fig. 16. Comparisons of hydrographs plotted at $x = 15$ km, for the cases that a finite channel with length 20 km, 50 km and a semi-infinite channel with upstream boundary, respectively; a pulse input from the lateral inflow concentrated at $x_0 = 10$ km.

lessened by the downstream boundary for a channel with length 20 km compared to a semi-infinite channel and that the effect of the downstream boundary vanishes provided the channel length exceeds 50 km.

3. Conclusions

In the present paper, we have systematically extended the results by Hayami [17], Dooge et al. [11], Moussa [19] and Singh [28] and expressed the general solutions of the diffusive wave model in a unified form in terms of *K*-function applicable for infinite, semi-infinite and finite channels with concentrated and uniform lateral inflows (as summarized in Table 2).

By using *Laplace* transform method, the integration of *K*-function, *S*-function, is obtained, which represents the flood routing process with a continuous unit input.

(1) Characteristics of $S_l(x,t)$, *S*-function for an infinite channel with uniform lateral inflow in the region $[x_1, x_2]$ are analyzed in detail. (a) $S_l(x,t)$ are negative for $x < x_1$ and approximates to zero as time tends to infinity; Each curve has a minimum which diminishes as x approaches to x_1; (b) $S_l(x,t)$ increases with t for $x > x_2$ and decreases with x; Each curve has the common limit, unit; (c) The limits of $S_l(x,t)$ rise with the coordinates for $x_1 < x < x_2$.

(2) $S_u(x,t)$ and $S_d(x,t)$ representing *S*-function for a semi-infinite channel with upstream inflow or downstream outflow are further examined, respectively. Both $S_u(x,t)$ and $S_d(x,t)$ are positive, implying the upstream inflow as well as downstream outflow enhance the discharge in a channel. The limits for $S_u(x,t)$ and $S_d(x,t)$ are unit and $\exp(Cx/D)$, respectively. It shows that the boundary conditions at two ends of a channel exert different influences on the $S_l(x,t)$, namely, the discharge from the lateral inflow input. The upstream boundary always amplifies the discharge, while the downstream boundary diminishes it. As time approaches to infinity, the limits of $S_l(x,t)$ in an infinite channel are the same as that in a semi-infinite channel with upstream boundary. However, comparing the limits of $S_l(x,t)$ in an infinite channel to that in a semi-infinite channel with

Table 2
Solutions obtained for various types of channel

Channel types	Solutions			
	Upstream boundary inflow	Downstream boundary outflow	Inputs from lateral inflow	
			Uniform	Concentrated
I			Eq. (18)—$K_l(x,t)$	Eq. (24)—$K_l(x,t)$ Eq. (25)—$S_l(x,t)$
SI-U	Eq. (36)—$S_u(x,t)$		Eq. (37)—$K_l(x,t)$	Eq. (38)—$K_l(x,t)$ Eq. (39)—$S_l(x,t)$
SI-D		Eq. (45)—$S_d(x,t)$	Eq. (37)—$K_l(x,t)$	Eq. (49)—$K_l(x,t)$ Eq. (50)—$S_l(x,t)$
F	Eq. (59)—$S_u(x,t)$	Eq. (60)—$S_d(x,t)$	Eq. (61)—$K_l(x,t)$ Eq. (62)—$S_l(x,t)$	Eq. (64)—$K_l(x,t)$ Eq. (65)—$S_l(x,t)$

Note: 'I' means infinite; 'SI-U' means semi-infinite with upstream boundary; 'SI-D' means semi-infinite with downstream boundary; 'F' means finite.

downstream boundary, we have a difference $\exp(Cx/D)$ which happens to be the limit of $S_{\mathrm{d}}(x,t)$. It exhibits the superposition of effects of lateral inflow and downstream boundary to some extent.

The discharge reduction in the upstream direction due to both downstream boundary and lateral inflow is usually called as backwater effect. In the present paper, hydrographs are used to observe the reduced discharge and hence to analyze the backwater effect. The backwater effect of the lateral inflow in an infinite channel is firstly investigated, which appears to have a maximum at the confluent point and then reduce as moving away from the confluent region in the upstream direction. Furthermore, we find that the backwater effect of lateral inflow is apparently affected by the boundary conditions. It shows that the upstream boundary alleviates the backwater effect of lateral inflow, while the downstream boundary enhances it.

Acknowledgements

The financial support from the National Natural Science Foundation of China under the grant 10332050 is appreciated. The authors also acknowledge the helpful comments provided by the anonymous reviewers.

Appendix A

By using transformation,

$$Q(x,t)=\exp\left(\frac{Cx}{2D}-\frac{C^2t}{4D}\right)\varphi(x,t) \tag{68}$$

the convection–diffusion equation (3) can be converted into a pure diffusion equation,

$$\frac{\partial\varphi}{\partial t}=D\frac{\partial^2\varphi}{\partial x^2}+\exp\left(-\frac{Cx}{2D}+\frac{C^2t}{4D}\right)f(x,t) \tag{69}$$

and the initial condition for an infinite channel Eq. (7) is transformed into,

$$\varphi(x,t)|_{t=0}=\varphi(x,0)=\exp\left(-\frac{Cx}{2D}\right)Q_0(x) \tag{70}$$

By using *Laplace* transform, Eq. (69) can be converted into,

$$\frac{\partial^2\tilde{\varphi}(x,p)}{\partial x^2}-\frac{p}{D}\tilde{\varphi}(x,p)=\frac{R(x,p)}{D},\quad -\infty<x<+\infty \tag{71}$$

in which,

$$\mathsf{L}[\varphi(x,t)]=\tilde{\varphi}(x,p),\quad \mathsf{L}[f(x,t)]=\tilde{f}(x,p)$$
$$\text{and}\quad \mathsf{L}[Q_{\mathrm{u}}(t)]=\tilde{Q}_{\mathrm{u}}(p) \tag{72}$$

$$R(x,p)=-\exp\left(-\frac{Cx}{2D}\right)\tilde{f}\left(x,p-\frac{C^2}{4D}\right)-\varphi(x,0) \tag{73}$$

Solution of this second order ordinary differential equation is,

$$\tilde{\varphi}(x,p)=-\frac{\sqrt{D}}{2\sqrt{p}}\int_{-\infty}^{x}\frac{R(\xi,p)}{D}\exp\left(-\sqrt{\frac{p}{D}}(x-\xi)\right)\mathrm{d}\xi -\frac{\sqrt{D}}{2\sqrt{p}}\int_{x}^{\infty}\frac{R(\xi,p)}{D}\exp\left(-\sqrt{\frac{p}{D}}(\xi-x)\right)\mathrm{d}\xi \tag{74}$$

Hence using the inverse *Laplace* transformation yields,

$$\varphi(x,t)=-\frac{1}{2\sqrt{\pi Dt}}\int_{-\infty}^{\infty}\mathsf{L}^{-1}[R(\xi,p)]*\exp\left(-\frac{(x-\xi)^2}{4Dt}\right)\mathrm{d}\xi \tag{75}$$

Substituting the above equation into Eq. (68) gives,

$$Q(x,t)=\int_{-\infty}^{\infty}Q_0(\xi)K_0(x,\xi,t)\,\mathrm{d}\xi+\int_{-\infty}^{\infty}f(\xi,t)*K_0(x,\xi,t)\,\mathrm{d}\xi \tag{76}$$

where,

$$K_0(x,\xi,t)=\exp\left(\frac{C(x-\xi)}{2D}-\frac{C^2t}{4D}\right)\times\frac{1}{2\sqrt{\pi Dt}}\exp\left(-\frac{(x-\xi)^2}{4Dt}\right)=\frac{1}{2\sqrt{\pi Dt}}\exp\left(-\frac{(x-\xi-Ct)^2}{4Dt}\right) \tag{77}$$

Appendix B

For semi-infinite channels with upstream boundary, the initial and boundary conditions are proposed as Eqs. (32) and (31) respectively. By using the same transformation as Eq. (68), the initial and boundary conditions are transformed into,

$$\varphi(x,t)|_{t=0}=\varphi(x,0)=\exp\left(-\frac{Cx}{2D}\right)Q_0(x) \tag{78}$$

$$\varphi(x,t)|_{x=0}=\varphi(0,t)=\exp\left(\frac{C^2t}{4D}\right)Q_{\mathrm{u}}(t) \tag{79}$$

By using *Laplace* transform, Eq. (69) can be converted into,

$$\frac{\partial^2\tilde{\varphi}(x,p)}{\partial x^2}-\frac{p}{D}\tilde{\varphi}(x,p)=\frac{R(x,p)}{D},\quad 0\leqslant x<+\infty \tag{80}$$

with boundary condition into,

$$\tilde{\varphi}(0,p)=\tilde{Q}_{\mathrm{u}}\left(p-\frac{C^2}{4D}\right) \tag{81}$$

in which,

$$\mathrm{L}[\varphi(x,t)] = \tilde{\varphi}(x,p), \quad \mathrm{L}[f(x,t)] = \tilde{f}(x,p) \quad \text{and} \quad \mathrm{L}[Q_u(t)] = \tilde{Q}_u(p) \tag{82}$$

$$R(x,p) = -\exp\left(-\frac{Cx}{2D}\right)\tilde{f}\left(x, p-\frac{C^2}{4D}\right) - \varphi(x,0) \tag{83}$$

Solution of this second order ordinary differential equation is,

$$\begin{aligned}\tilde{\varphi}(x,p) = {} & \tilde{Q}_u\left(p-\frac{C^2}{4D}\right)\exp\left(-\sqrt{\frac{p}{D}}x\right) \\ & + \frac{\sqrt{D}}{2\sqrt{p}}\int_0^\infty \frac{R(\xi,p)}{D}\exp\left(-\sqrt{\frac{p}{D}}(\xi+x)\right)\mathrm{d}\xi \\ & - \frac{\sqrt{D}}{2\sqrt{p}}\int_0^x \frac{R(\xi,p)}{D}\exp\left(-\sqrt{\frac{p}{D}}(x-\xi)\right)\mathrm{d}\xi \\ & - \frac{\sqrt{D}}{2\sqrt{p}}\int_x^\infty \frac{R(\xi,p)}{D}\exp\left(-\sqrt{\frac{p}{D}}(\xi-x)\right)\mathrm{d}\xi\end{aligned} \tag{84}$$

Using the inverse *Laplace* transformation gives,

$$\begin{aligned}\varphi(x,t) = {} & \left[Q_u(t)\exp\left(\frac{C^2t}{4D}\right)\right] * \left[\frac{x}{2\sqrt{\pi Dt^3}}\exp\left(-\frac{x^2}{4Dt}\right)\right] \\ & + \frac{1}{2\sqrt{\pi Dt}}\int_0^\infty \mathrm{L}^{-1}[R(\xi,p)] * \exp\left(-\frac{(x+\xi)^2}{4Dt}\right)\mathrm{d}\xi \\ & - \frac{1}{2\sqrt{\pi Dt}}\int_0^\infty \mathrm{L}^{-1}[R(\xi,p)] * \exp\left(-\frac{(x-\xi)^2}{4Dt}\right)\mathrm{d}\xi\end{aligned} \tag{85}$$

Solution of the original equation is therefore obtained by substituting the above equation into Eq. (68) as follows:

$$Q(x,t) = Q_u(t) * K_u(x,t) + \int_0^\infty Q_0(\xi)K_0(x,\xi,t)\,\mathrm{d}\xi + \int_0^\infty f(\xi,t) * K_0(x,\xi,t)\,\mathrm{d}\xi \tag{86}$$

where,

$$\begin{aligned}K_u(x,t) &= \exp\left(\frac{Cx}{2D}-\frac{C^2t}{4D}\right)\frac{x}{2\sqrt{\pi D}t^{3/2}}\exp\left(-\frac{x^2}{4Dt}\right) \\ &= \frac{x}{2\sqrt{\pi D}t^{3/2}}\exp\left(-\frac{(x-Ct)^2}{4Dt}\right)\end{aligned} \tag{87}$$

$$\begin{aligned}K_0(x,\xi,t) &= \exp\left(\frac{C(x-\xi)}{2D}-\frac{C^2t}{4D}\right)\frac{1}{2\sqrt{\pi Dt}} \\ &\quad \times \left[\exp\left(-\frac{(x-\xi)^2}{4Dt}\right) - \exp\left(-\frac{(x+\xi)^2}{4Dt}\right)\right] \\ &= \frac{1}{2\sqrt{\pi Dt}}\left[\exp\left(-\frac{(x-\xi-Ct)^2}{4Dt}\right) - \exp\left(\frac{Cx}{D}\right)\exp\left(-\frac{(x+\xi+Ct)^2}{4Dt}\right)\right]\end{aligned} \tag{88}$$

Appendix C

For a semi-infinite channel with downstream boundary, the governing equation, initial and boundary conditions are defined as Eqs. (3), (42) and (41). Solution for Eq. (80) in region $(-\infty, 0]$ is,

$$\begin{aligned}\tilde{\varphi}(x,p) = {} & \tilde{Q}_d\left(p-\frac{C^2}{4D}\right)\exp\left(\sqrt{\frac{p}{D}}x\right) \\ & + \frac{\sqrt{D}}{2\sqrt{p}}\int_{-\infty}^0 \frac{R(\xi,p)}{D}\exp\left(\sqrt{\frac{p}{D}}(x+\xi)\right)\mathrm{d}\xi \\ & + \frac{\sqrt{D}}{2\sqrt{p}}\int_0^x \frac{R(\xi,p)}{D}\exp\left(\sqrt{\frac{p}{D}}(x-\xi)\right)\mathrm{d}\xi \\ & - \frac{\sqrt{D}}{2\sqrt{p}}\int_{-\infty}^x \frac{R(\xi,p)}{D}\exp\left(-\sqrt{\frac{p}{D}}(x-\xi)\right)\mathrm{d}\xi\end{aligned} \tag{89}$$

By applying the inverse *Laplace* transformation we have,

$$\begin{aligned}\varphi(x,t) = {} & \left[Q_d(t)\exp\left(\frac{C^2t}{4D}\right)\right] * \left[\frac{-x}{2\sqrt{\pi Dt^3}}\exp\left(-\frac{x^2}{4Dt}\right)\right] \\ & + \frac{1}{2\sqrt{\pi Dt}}\int_{-\infty}^0 \mathrm{L}^{-1}[R(\xi,p)] * \exp\left(-\frac{(x+\xi)^2}{4Dt}\right)\mathrm{d}\xi \\ & - \frac{1}{2\sqrt{\pi Dt}}\int_{-\infty}^0 \mathrm{L}^{-1}[R(\xi,p)] * \exp\left(-\frac{(x-\xi)^2}{4Dt}\right)\mathrm{d}\xi\end{aligned} \tag{90}$$

Thus substituting the above equation into Eq. (68) gives the solution as,

$$Q(x,t) = Q_d(t) * K_d(x,t) + \int_{-\infty}^0 Q_0(\xi)K_0(x,\xi,t)\,\mathrm{d}\xi + \int_{-\infty}^0 f(\xi,t) * K_0(x,\xi,t)\,\mathrm{d}\xi \tag{91}$$

where,

$$\begin{aligned}K_d(x,t) &= \exp\left(\frac{Cx}{2D}-\frac{C^2t}{4D}\right)\frac{|x|}{2\sqrt{\pi D}t^{3/2}}\exp\left(-\frac{x^2}{4Dt}\right) \\ &= \frac{|x|}{2\sqrt{\pi D}t^{3/2}}\exp\left(-\frac{(|x|+Ct)^2}{4Dt}\right)\end{aligned} \tag{92}$$

and $K_0(x,\xi,t)$ identical to Eq. (88).

Appendix D

For a finite channel the initial and boundary conditions are proposed as Eqs. (54) and (53). By taking the same transformation as Eq. (68), the initial and boundary conditions are converted into,

$$\varphi(x,t)|_{t=0} = \exp\left(-\frac{Cx}{2D}\right)Q_0(x) \tag{93}$$

$$\varphi(x,t)|_{x=0} = \exp\left(\frac{C^2t}{4D}\right)Q_u(t),\quad \varphi(x,t)|_{x=L} = \exp\left(-\frac{CL}{2D}+\frac{C^2t}{4D}\right)Q_d(t) \tag{94}$$

The boundary conditions of this problem are still inhomogeneous. Considering such transformation,

$$\phi(x,t) = \varphi(x,t) - \frac{L-x}{L}\exp\left(\frac{C^2t}{4D}\right)Q_u(t) - \frac{x}{L}\exp\left(-\frac{CL}{2D}+\frac{C^2t}{4D}\right)Q_d(t) \tag{95}$$

we have a problem with homogeneous boundary conditions. The governing equation is accordingly as,

$$\frac{\partial\phi}{\partial t} = D\frac{\partial^2\phi}{\partial x^2} + F_s(x,t) \tag{96}$$

in which,

$$\begin{aligned}F_s(x,t) &= \exp\left(-\frac{Cx}{2D}+\frac{C^2t}{4D}\right)f(x,t) - \frac{C^2}{4D}\frac{L-x}{L}\exp\left(\frac{C^2t}{4D}\right)Q_u(t)\\ &\quad - \frac{C^2}{4D}\frac{x}{L}\exp\left(-\frac{CL}{2D}+\frac{C^2t}{4D}\right)Q_d(t) - \frac{L-x}{L}\exp\left(\frac{C^2t}{4D}\right)\frac{dQ_u(t)}{dt}\\ &\quad - \frac{x}{L}\exp\left(-\frac{CL}{2D}+\frac{C^2t}{4D}\right)\frac{dQ_d(t)}{dt}\end{aligned} \tag{97}$$

and the initial and boundary conditions are,

$$\phi(x,t)|_{t=0} = \phi(x,0) \tag{98}$$

$$\phi(x,t)|_{x=0} = 0,\quad \phi(x,t)|_{x=L} = 0 \tag{99}$$

where,

$$\phi(x,0) = \exp\left(-\frac{Cx}{2D}\right)Q_0(x) - \frac{L-x}{L}Q_u(0) - \frac{x}{L}\exp\left(-\frac{CL}{2D}\right)Q_d(0) \tag{100}$$

Solution of this problem can be obtained by the separation of variables method,

$$\phi(x,t) = \sum_n\left\{\exp\left(-\left(\frac{n\pi}{L}\right)^2Dt\right) * \left[F_n(t)+\phi_n\delta(t)\right]\right\}\sin\left(\frac{n\pi x}{L}\right) \tag{101}$$

in which the *Fourier* coefficients are,

$$F_n(t) = \frac{2}{L}\int_0^L F_s(x,t)\sin\left(\frac{n\pi x}{L}\right)dx \tag{102}$$

$$\phi_n = \frac{2}{L}\int_0^L \phi(x,0)\sin\left(\frac{n\pi x}{L}\right)dx \tag{103}$$

By substituting Eq. (101) into Eq. (95) we have,

$$\begin{aligned}\varphi(x,t) &= \sum_n\left\{\exp\left(-\left(\frac{n\pi}{L}\right)^2Dt\right) * [F_n(t)+\phi_n\delta(t)]\right\}\sin\left(\frac{n\pi x}{L}\right)\\ &\quad + \frac{L-x}{L}\exp\left(\frac{C^2t}{4D}\right)Q_u(t) + \frac{x}{L}\exp\left(-\frac{CL}{2D}+\frac{C^2t}{4D}\right)Q_d(t)\end{aligned} \tag{104}$$

Finally substituting the above equation to Eq. (68) gives,

$$\begin{aligned}Q(x,t) &= Q_u(t) * K_u(x,t) + Q_d(t) * K_d(x,t) + \int_0^L Q_0(\xi)K_0(x,\xi,t)\,d\xi\\ &\quad + \int_0^L f(\xi,t) * K_0(x,\xi,t)\,d\xi\end{aligned} \tag{105}$$

in which,

$$K_u(x,t) = \exp\left(\frac{Cx}{2D}-\frac{C^2t}{4D}\right)\sum_{n=1}^{+\infty}\frac{2n\pi D}{L^2}\times\exp\left(-\frac{n^2\pi^2D}{L^2}t\right)\sin\frac{n\pi x}{L} \tag{106}$$

$$K_d(x,t) = \exp\left(\frac{C(x-L)}{2D}-\frac{C^2t}{4D}\right)\sum_{n=1}^{+\infty}\frac{2n\pi D}{L^2}(-1)^{n+1}\times\exp\left(-\frac{n^2\pi^2D}{L^2}t\right)\sin\frac{n\pi x}{L} \tag{107}$$

$$K_0(x,\xi,t) = \exp\left(\frac{C(x-\xi)}{2D}-\frac{C^2t}{4D}\right)\frac{2}{L}\sum_{n=1}^{+\infty}\exp\left(-\frac{n^2\pi^2D}{L^2}t\right)\times\sin\frac{n\pi\xi}{L}\sin\frac{n\pi x}{L} \tag{108}$$

Appendix E

In Fig. 17, a channel with a tributary with a rectangular cross section is illustrated, in which the width of main stem and tributary are B and B_l, respectively. The discharge in the main stem and tributary are denoted by Q and Q_l, respectively. The confluent angle is θ. L represents the length of the confluent area. The cell with lateral inflow is considered, length of which is dx. In a time interval dt, the net volume of the water for this cell, namely, the difference between the outflow at the right border of the cell and inflow at the left border, should be $(\partial Q/\partial x)\,dx\,dt$. The lateral inflow is $(Q_l/B_l)\sin\theta\,dx\,dt$. The increment of the water for the cell is $(\partial h/\partial t)B\,dx\,dt$. Hence, in line with the conservation law of the water, there satisfies,

$$\frac{\partial h}{\partial t}B\,dx\,dt + \frac{\partial Q}{\partial x}dx\,dt = \frac{Q_l}{B_l}\sin\theta\,dx\,dt \tag{109}$$

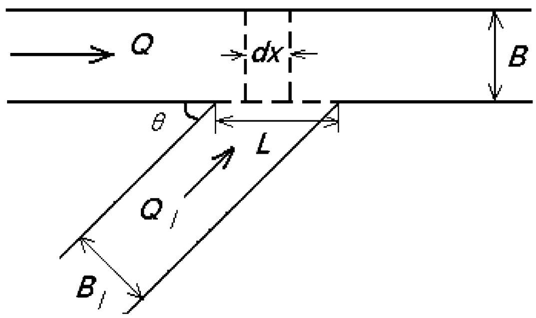

Fig. 17. Sketch for a channel with a tributary.

As $Q = qB$, then the continuity equation can be readily obtained as following:

$$\frac{\partial h}{\partial t} + \frac{\partial q}{\partial x} = \frac{q_1}{B} \tag{110}$$

or,

$$\frac{\partial A}{\partial t} + \frac{\partial Q}{\partial x} = q_1 \tag{111}$$

where Q denotes the discharge, A is the wetted surface, $q_1 = (Q_1/B_1)\sin\theta$. Similarly, the net momentum for this cell in a time interval $\mathrm{d}t$ should be $[\partial(Qq/h)/\partial x]\mathrm{d}x\,\mathrm{d}t$. The velocity component of the lateral inflow in the flow direction of the mainstream is $u_1 = (Q_1/B_1)/\cos\theta/h$. Thus, the momentum of the lateral inflow in a time interval $\mathrm{d}t$ is $(Q_1/B_1)\sin\theta(Q_1/h/B_1)/\cos\theta\,\mathrm{d}x\,\mathrm{d}t$. The impulse in the flow direction made by the water weight, the frictional resistance and water pressures are $BghS_0\mathrm{d}x\,\mathrm{d}t$, $-BghS_\mathrm{f}\mathrm{d}x\,\mathrm{d}t$, and $[\partial(gh^2/2)/\partial x]B\,\mathrm{d}x\,\mathrm{d}t$, respectively. The increment of the momentum for the cell is $(\partial Q/\partial t)\mathrm{d}x\,\mathrm{d}t$. Therefore, according to the conservation law of the momentum, we have,

$$\frac{\partial Q}{\partial t}\mathrm{d}x\,\mathrm{d}t + \frac{\partial}{\partial x}\left(Q\frac{q}{h} + B\frac{gh^2}{2}\right)\mathrm{d}x\,\mathrm{d}t = Bgh(S_0 - S_\mathrm{f})\,\mathrm{d}x\,\mathrm{d}t + \frac{Q_1}{B_1}\sin\theta\frac{Q_1}{hB_1}\cos\theta\,\mathrm{d}x\,\mathrm{d}t \tag{112}$$

which can be simplified into,

$$\frac{\partial q}{\partial t} + \frac{\partial}{\partial x}\left(\frac{q^2}{h} + \frac{gh^2}{2}\right) = gh(S_0 - S_\mathrm{f}) + \frac{q_1}{B}u_1 \tag{113}$$

The above equation is the momentum equation of conservative form. As $q = hv$, the above equation can be also rewritten into,

$$h\frac{\partial v}{\partial t} + v\frac{\partial h}{\partial t} + 2hv\frac{\partial v}{\partial x} + v^2\frac{\partial h}{\partial x} + gh\frac{\partial h}{\partial x} = gh(S_0 - S_\mathrm{f}) + \frac{q_1}{B}u_1 \tag{114}$$

Likewise, the continuity equation can be transformed into,

$$\frac{\partial h}{\partial t} + v\frac{\partial h}{\partial x} + h\frac{\partial v}{\partial x} = \frac{q_1}{B} \tag{115}$$

Therefore we can obtain the momentum equation of the non-conservative form as below,

$$\frac{\partial v}{\partial t} + v\frac{\partial v}{\partial x} + g\frac{\partial h}{\partial x} = g(S_0 - S_\mathrm{f}) + \frac{q_1(u_1 - v)}{Bh} \tag{116}$$

which is identical to that described by Singh [28].

Let v_0, h_0 denote the typical velocity and flow depth, and we can acquire the non-dimensional variables as following:

$$\bar{x} = \frac{x}{h_0},\quad \bar{t} = \frac{v_0 t}{h_0},\quad \bar{v} = \frac{v}{v_0},\quad \bar{h} = \frac{h}{h_0},\quad \bar{q} = \frac{q}{v_0 h_0},\quad \bar{q}_1 = \frac{q_1}{v_0 h_0},\quad \bar{u}_1 = \frac{u_1}{v_0} \tag{117}$$

Then Eqs. (110), (113) and (116) can be transform to

$$\frac{\partial \bar{h}}{\partial \bar{t}} + \frac{\partial(\bar{h}\bar{v})}{\partial \bar{x}} = \frac{\bar{q}_1}{B} \tag{118}$$

$$\frac{v_0^2}{gh_0}\left[\frac{\partial \bar{q}}{\partial \bar{t}} + \frac{\partial}{\partial \bar{x}}\left(\frac{\bar{q}^2}{\bar{h}}\right) - \frac{\bar{q}_1}{\bar{B}}\bar{u}_1\right] + \bar{h}\frac{\partial \bar{h}}{\partial \bar{x}} = \bar{h}(S_0 - S_\mathrm{f}) \tag{119}$$

$$\frac{v_0^2}{gh_0}\left[\frac{\partial \bar{v}}{\partial \bar{t}} + v\frac{\partial \bar{v}}{\partial \bar{x}} - \frac{\bar{q}_1(\bar{u}_1 - \bar{v})}{\bar{B}\bar{h}}\right] + \frac{\partial \bar{h}}{\partial \bar{x}} = (S_0 - S_\mathrm{f}) \tag{120}$$

With assumption of sub-critical flow condition, $Fr^2 = (v_0)^2/(gh_0) \ll 1$, the momentum equation can be simplified as,

$$\frac{\partial h}{\partial x} = (S_0 - S_\mathrm{f}) \tag{121}$$

in which the terms of inertia are negligible. In addition, the relation of *Chézy* is known as,

$$S_\mathrm{f} = \frac{Q^2}{K^2} \tag{122}$$

where the conveyance of the channel is taken as,

$$K(h) = CR_\mathrm{h}^{1/2}A \tag{123}$$

in which C is the *Chézy* coefficient, and R_h is the hydraulic radius. The momentum equation can also be written as [16],

$$\frac{\partial h}{\partial x} - S_0 + \frac{Q^2}{K^2} = 0 \tag{124}$$

and the continuity equation can be rewritten to

$$\frac{\partial h}{\partial t} + \frac{1}{B}\frac{\partial Q}{\partial x} = \frac{q_1}{B} \tag{125}$$

Differentiating the above equation with respect to x, yields,

$$\frac{\partial^2 h}{\partial x \partial t} + \frac{1}{B}\frac{\partial^2 Q}{\partial x^2} = \frac{1}{B}\frac{\partial q_1}{\partial x} \tag{126}$$

Differentiating the equation of motion with respect to t, and assuming $\partial S_0/\partial t = 0$, yields,

$$\frac{\partial^2 h}{\partial x \partial t} + \frac{2Q}{K^2}\frac{\partial Q}{\partial t} - \frac{2Q^2}{K^3}\frac{\partial K}{\partial t} = 0 \tag{127}$$

According to the continuity equation, we have,

$$\frac{\partial K}{\partial t} = \frac{dK}{dh}\frac{\partial h}{\partial t} = \frac{1}{B}\frac{dK}{dh}\left(q_1 - \frac{\partial Q}{\partial x}\right) \tag{128}$$

Eliminating the term $\partial^2 h/\partial x \partial t$ from Eqs. (126) and (127) renders a single equation,

$$\frac{\partial Q}{\partial t} + \frac{Q}{BK}\frac{dK}{dh}\frac{\partial Q}{\partial x} - \frac{K^2}{2BQ}\frac{\partial^2 Q}{\partial x^2} = \frac{Q}{BK}\frac{dK}{dh}q_1 - \frac{K^2}{2BQ}\frac{\partial q_1}{\partial x} \tag{129}$$

This is the equation of diffusive wave, with only one dependent variable, Q. The celerity and the diffusion coefficient are respectively,

$$C = \frac{Q}{BK}\frac{dK}{dh} = \frac{1}{B}\frac{dQ}{dh} \tag{130}$$

$$D = \frac{K^2}{2BQ} = \frac{Q}{2BS_f} \tag{131}$$

Therefore, the diffusive wave equation can now be written as,

$$\frac{\partial Q}{\partial t} + C\frac{\partial Q}{\partial x} - D\frac{\partial^2 Q}{\partial x^2} = Cq_1 - D\frac{\partial q_1}{\partial x} \tag{132}$$

References

[1] Abbott MB. An introduction to the method of characteristics. New York: Elsevier; 1966.

[2] Abbott MB. Computational hydraulics. London: Pitman; 1979.

[3] Barry DA, Bajracharya K. On the Muskingum–Cunge flood routing method. Environ Int 1995;21:485–90.

[4] Bajracharya K, Barry DA. Accuracy criteria for linearised diffusion wave flood routing. J Hydrol 1997;195:200–17.

[5] Cappelaere B. Accurate diffusive wave routing. J Hydraul Eng, ASCE 1997;123:174–81.

[6] Cunge J, Holly FM, Verwey A. Practical aspects of computational river hydraulics. London: Pitman Advanced Publishing Program; 1980.

[7] Chung WH, Aldama AA, Smith JA. On the effects of downstream boundary conditions on diffusive flood routing. Adv Water Resour 1993;16:259–75.

[8] Daluz Vieira JH. Conditions governing the use of approximations for the Saint-Venant equations for shallow water flow. J Hydrol 1983;60:43–58.

[9] Dooge JCI. A general theory of the unit hydrograph. J Geophys Res 1959;64:241–56.

[10] Dooge JCI, Harley BM. Linear routing in uniform channels. Proc. Int. Hydrol Symp. Fort Collins, CO: Colorado State University; 1967.

[11] Dooge JCI, Kundzewicz ZW, Napiorkowski JJ. On backwater effects in linear diffusion routing. Hydrol Sci J 1983;28:391–402.

[12] Dooge JCI, Napiorkowski JJ. Effects of downstream control in diffusion routing. Acta Geophis Polon 1984;32:363–73.

[13] Fan P, Li JC, Liu QQ. Influences of the shrink of dividing channels and the DongTing Lake on the flood in the Yangzte River. Mech Eng (in Chinese) 2004;26:17–21.

[14] Fan P, Li JC, Liu QQ. Diffusive waves in a channel with concentrated lateral inflow. In: Recent advances in fluid mechanics, Proc the 4th international conference on fluid mechanics, Dalian, China, 2004. p. 347–50.

[15] Fread D. Flood routing. In: Anderson MG, Burt TP, editors. Hydrological forecasting. Chichester: Wiley; 1985.

[16] Graf WH. Fluvial hydraulics: flow and transport processes in channels of simple geometry. Chichester: John Wiley & Sons Ltd.; 1998.

[17] Hayami S. On the propagation of flood waves. Disaster Prev Res Inst Bull 1951;1:1–16.

[18] Moramarco T, Fan Y, Bras RL. Analytical solution for channel routing with uniform lateral inflow. ASCE, J Hydraul Eng 1999;125:707–13.

[19] Moussa R. Analytical Hayami solution for the diffusive wave flood routing problem with lateral inflow. Hydrol Process 1996; 10:1209–27.

[20] Moussa R, Bocquillon C. Criteria for the choice of flood-routing methods in natural channels. J Hydrol 1996;186:1–30.

[21] Perkins SP, Koussis AD. Stream-aquifer interaction model with diffusive wave routing. J Hydraul Eng, ASCE 1996;122:210–8.

[22] Ponce VM, Simons DB. Shallow wave propagation in open channel flow. J Hydraul Div ASCE 1977;103:1461–76.

[23] Ponce VM, Li RM, Simons DB. Applicability of kinematic and diffusion models. J Hydraul Div ASCE 1978;104:353–60.

[24] Ponce VM. Engineering hydrology, principles and practices. Englewood Cliffs, NJ: Prentice Hall; 1989.

[25] Ponce VM. Generalized diffusive wave equation with inertial effects. Water Resour Res 1990;26:1099–101.

[26] Singh VP. Accuracy of kinematic wave and diffusion wave approximations for space-independent flows. Hydrol Process 1994;8:45–62.

[27] Singh VP. Accuracy of kinematic wave and diffusion wave approximations for time-independent flows. Hydrol Process 1995;9:755–82.

[28] Singh VP. Kinematic wave modeling in water resources: surface-water hydrology. New York: John Wiley & Sons Ltd.; 1996.

[29] Tan WY. Computing hydrodynamics for shallow water—application of the finite volume method. Beijing: Tsinghua University Press; 1998 [in Chinese].

[30] Tawatchai TM, Shyam KM. Analytical diffusion model for flood routing. J Hydraul Eng 1985;111:435–54.

[31] Tsai CW. Flood routing in mild-slope rivers-wave characteristics and downstream backwater effect. J Hydrol 2005;308:151–67.

[32] Venetis C. The IUH of the Muskingum channel reach. J Hydrol 1969;7:444–7.

[33] Weinmann PE, Laurenson EM. Approximate flood routing methods: a review. J Hydraul Div ASCE 1974;105:1521–36.